Session 2: Radial velocity surveys

Tenth anniversary of 51 Peg-b : Status of and prospects for hot Jupiter studies
Proceedings of Haute Provence Observatory Colloquium (22-25 August 2005)
Edited by L. Arnold, F. Bouchy, and C. Moutou

N2K: a targeted search for hot Jupiters

D. A. Fischer[1], G. Laughlin[2], G. W. Marcy[3], R. P. Butler[4], and S. S. Vogt[2]

[1]*Dept Physics & Astronomy, 1600 Holloway, San Francisco State University, San Francisco, CA 94132 [fischer@stars.sfsu.edu]*

[2] *UCO/Lick Observatory, University of California at Santa Cruz, Santa Cruz, CA 95064*

[3]*Dept Astronomy, 601 Campbell Hall, UC Berkeley, Berkeley, CA 94720*

[4]*Department of Terrestrial Magnetism, Carnegie Institute of Washington DC, 5241 Broad Branch Rd. NW, Washington DC, USA 20015-1305*

Abstract. The N2K consortium is carrying out a distributed observing campaign to detect short-period planets using the Keck, Magellan and Subaru telescopes, as well as the automatic photometric telescopes at Fairborn Observatory. We have established a reservoir of more than 14,000 main sequence and subgiant stars, closer than 110 pc, brighter than V=10.5 and with $0.4 < B - V < 1.2$. Because the fraction of stars with planets is a sensitive function of stellar metallicity, we are selecting a subset of about 2000 high metallicity stars for this program. Four short-period planets have been detected in the past year: HD 88133b, HD 149143b, HD 109749b and HD 149026. Among these new exoplanets, HD 149026b is a transiting planet with a 70 $M_\oplus$ mass heavy element core.

1. Introduction

This celebration of the 10 year anniversary of 51 Peg is a good time to reflect on the importance of short-period planets. Twenty nine of the nearly 160 known extrasolar planets have orbital periods that like 51 Peg, are shorter than 5 days. Astronomers are still trying to under-

stand the formation and evolution of these so-called hot Jupiter systems. What propels inward migration? How does migration stop and leave the planet parked in a stable orbit?

Short-period planets provide more information than any other class of extrasolar planets, at least until direct imaging missions launch. These systems offer the opportunity to observe polarized light or the reflected light spectrum of the planet. The distribution of orbital properties also offers clues about migration in these systems.

The most exciting characteristic of hot Jupiter planets is the increased probability for observing transits. Transiting planets around bright stars provide information about the structure and atmosphere of extrasolar planets that is otherwise impossible to obtain. There are now four examples of planets that transit bright stars. The first discovery, HD 209458b (Charbonneau et al. 2000, Henry et al. 2000), revealed a bloated planet radius with neutral sodium detected in the dense lower atmosphere (Charbonneau et al. 2002) and an evaporating, trailing extended exosphere of hydrogen (Vidal-Madjar et al. 2004). Timing measurements of the secondary eclipse were made with the Spitzer Space telescope (Deming et al. 2005) and constrain the orbital eccentricity of HD209458b to be less than 0.02. TrES-1 was the second transiting planet, discovered around a $V = 11.8$ star. Photometric observations (Alonso et al. 2004) demonstrate that the planet has a radius similar to Jupiter. Observations of the secondary eclipse with the Spitzer Telescope place limits on the Bond albedo for TrES-1 (Charbonneau et al. 2005a) and constrain the orbital eccentricity to less than 0.01. The detection of the third a transiting planet around a bright star was made by Sato et al. (2005) and reveal a Saturn-mass planet with a radius of only 0.72 $R_{\rm Jup}$ orbiting HD 149026. Theoretical models of the interior structure of HD 149026b suggest the presence of a substantial ~ 70 $M_{\oplus}$ core (Sato et al. 2005, Fortney et al. 2005). The most recent addition to the list of transiting planets around bright stars is the K1V star, HD 189733, with a jovian mass planet (Bouchy et al. 2005). Like HD 209458, this planet has a radius of 1.26 $R_{\rm Jup}$, significantly larger than Jupiter. The transiting systems detected so far exhibit surprising diversity in the interior structure of extrasolar planets.

2. N2K Consortium

While hot Neptunes represent an important new parameter space for ongoing Doppler programs, virtually all short-period planets with $M \sin i$ greater than 0.5 $M_{\rm Jup}$ have been culled from long term Doppler planet surveys. The scientific value of hot Jupiters motivated the N2K

survey (and a similar metallicity-biased search at Haute Provence Observatory) aimed specifically at the detection of short-period planets.

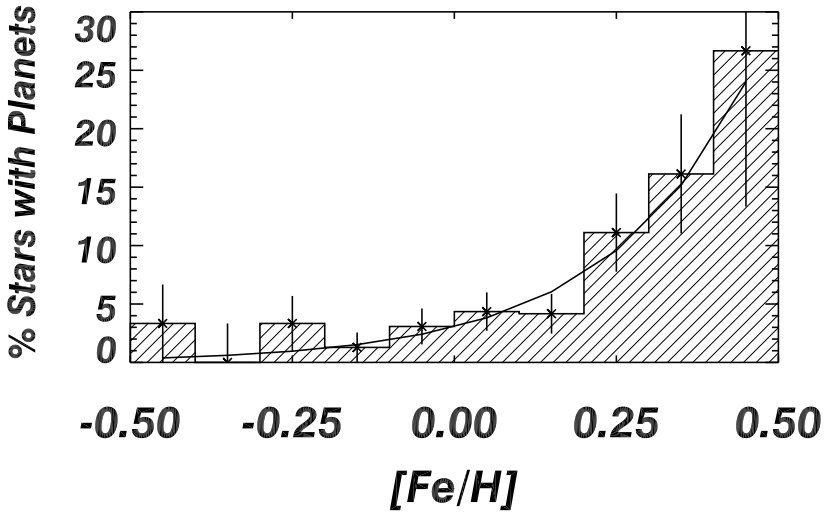

Figure 1. *The percentage of stars with detected planets rises with iron abundance (Fischer & Valenti 2005) and is well-fit with a power law.*

The N2K consortium (Fischer et al. 2005) is a partnership between U.S. astronomers (Keck), Chilean astronomers (Magellan) and Japanese astronomers (Subaru) to carry out a distributed Doppler survey for short-period planets around 2000 stars not on current Doppler programs. The database is a reservoir of more than 14,000 stars closer than 110 pc, with $0.45 < B - V < 1.2$, and brighter than $V = 10.5$. Initial metallicity estimates for all stars were made using a broadband color calibration (Ammons et al. 2005), and information regarding stellar multiplicity was culled from the Hipparcos catalog and the Double Star catalog.

As telescope time is allocated at Keck, Magellan and Subaru, an appropriate set of about 100 stars is drawn from the N2K database and observations are made over three consecutive nights. The correlation between metallicity of the host stars and the presence of extrasolar planets has been well-established (Gonzales 1998; Santos et al. 2001, 2005, Fischer, Valenti, & Marcy, 2003). From Figure 1 (Fischer &

Valenti 2005) it is clear that planet occurrence is sensitively dependent on stellar metallicity:

$$\mathcal{P}(\text{planet}) = 0.03 \times \left(\frac{(\mathrm{N_{Fe}/N_H})}{(\mathrm{N_{Fe}/N_H})_\odot} \right)^2$$

Stars with metallicity that is three times that of the Sun, have about four times as many gas giant planets as solar metallicity stars. Exploiting this correlation, the N2K target lists are biased toward high metallicity to boost the detection probability.

Monte Carlo simulations show that an RMS scatter between 15 and 100 m s^{-1} in the first three radial velocities, obtained on consecutive nights, is a good diagnostic for the presence of a short-period planet. For example, the first set of 230 stars observed at Keck yield an RMS velocity distribution shown in Figure 2. Spectroscopic binaries are easily identified by virtue of RV variations of several hundred kilometers per second (or more) over three nights. The cross-hatched region in Figure 2 identifies about 35 planet candidates. Once a planet candidate is identified from these initial 3 radial velocity measurements, follow-up Doppler and photometric observations are initiated to monitor the star for transits.

The primary goal of the N2K program is to identify planet candidates with suggestive RMS velocity scatter. However, we also measure chromospheric activity from the Ca H&K lines and carry out a spectroscopic analysis to derive effective temperature, surface gravity and metallicity from the high resolution spectra (following the method described in Valenti & Fischer 2005). The metallicity distribution of the 230 stars in Figure 2, allowed us to estimate the fraction of planets expected using the probability distribution shown in Figure 1. Given the metallicity distribution of our observed stars, we determined that 4 ± 2 hot Jupiters should have been detected. Indeed, three new short-period planets were identified in the 230 star sample, consistent with our prediction of 4 ± 2. In addition, there are 35 planet candidates that still need additional observations to establish the presence of (probably longer period) planets.

In the past year, the N2K consortium has identified four short period planets orbiting HD 88133 (Fischer et al. 2005), HD149026 (Sato et al. 2005), HD 149143 and HD 109749 (Fischer et al. 2005). The Keplerian fits for these last two planets, announced at this conference, are shown in Figures 3a and 3b.

HD 149143 is a metal-rich, chromospherically inactive GO IV star with a stellar radius of 1.49 $R_\odot$. Observations at Keck detected a planet of $M \sin i = 1.33\ M_{\rm Jup}$and an orbital period of 4.072 d. Photometric observations of HD 149143 were carried out with the automated photo-

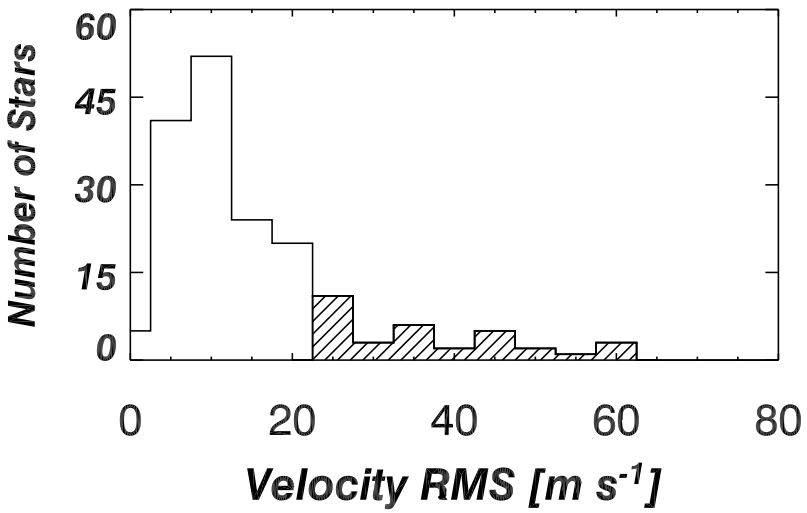

Figure 2. *Velocity scatter less than 80 m* s^{-1} *is observed for 175 of 230 stars observed at Keck after 3 or more RV observations. RV scatter less than* 3σ *is seen for 148 of these stars. However 35 stars, or 16% of the observed sample (indicated in the cross-hatched bins) show RV scatter, consistent with the presence of a planetary companion.*

metric telescopes at Fairborn Observatory. The photometry shows that the star is photometrically constant and rules out orbital inclinations greater than 83 degrees.

HD 109749 is a G3 IV star with [Fe/H] = 0.25 and a stellar radius of 1.24 $R_{\odot}$. The Keck velocities for this stars reveal a planet with an orbital period of 5.22 d and $M \sin i = 0.28\ M_{\rm Jup}$. Photometric follow-up of this star was obtained with the SMARTS consortium telescope, the PROMPT telescope and by amateur astronomers participating in `transitsearch.org` in Adelaide and South Africa. None of these photometric data detected a decrement in brightness at the expected transit time and constrain the orbital inclination to less than 85 degrees for gas giant planets with radii down to 0.7 $R_{\rm Jup}$.

Transit follow-up observations have been made for all four short-period systems and rule out the presence of transits down to a $\sim$ 1 millimag photometric depth in HD 88133, HD 149143 and HD 109749.

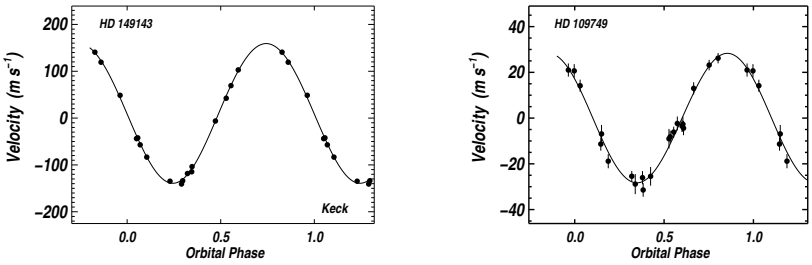

Figure 3. *(a) Phased radial velocities for HD 149143 are plotted with a Keplerian model (solid line) for a planet with an orbital period of* 4.072 ± 0.7 *d,* $M \sin i = 1.33\ M_{\rm Jup}$ *and circular orbit with an orbital radius of 0.053 AU. (b) Phased radial velocities for HD 109749. With an orbital period of 5.24 d, velocity amplitude of 28.7 m* s^{-1} *and stellar mass of 1.2* $M_{\odot}$ *we derive a planet mass,* $M \sin i = 0.28\ M_{\rm Jup}$ *and orbital radius of 0.0635 AU.*

3. HD 149026

Keck follow up observations of one of the Subaru candidates, HD 149026, revealed a Saturn-mass planet that was subsequently observed to transit its host star (Sato et al. 2005).

HD 149026 is a $V = 8.15$ G0 IV metal rich star with $v \sin i = 6.0 \pm 0.5$ km s^{-1} with a stellar radius of $1.45 \pm 0.1\ R_{\odot}$. The Yale evolutionary tracks (DeMarque et al. 2004) yield a stellar mass of $1.3 \pm 0.1\ M_{\odot}$. The orbital period for this stars is $P = 2.877 \pm 0.001$ day. We adopt a fixed circular orbit (consistent with the data) and derive $M \sin i = 0.36\ M_{\rm Jup}$, and $a_{\rm rel} = 0.042$ AU for HD 149026b.

Surprisingly, 4 of the first 7 Keck radial velocities were serendipitously obtained in transit (Figure 4). The four radial velocities obtained during transit exhibit the Rossiter-McLaughlin effect, a deviation from Keplerian velocities which occurs because a transiting planet occults first the approaching limb of the rotating star and then the receding limb of the star. If the orbital plane is coplanar with the stellar equatorial plane, then a symmetrical deviation occurs about mid-transit. The observation of this effect in the Doppler velocities was an annoyance for purposes of modeling a single planet, but provided an unambiguous and independent confirmation of the photometric planet transit. Additional radial velocities have been obtained at Keck during transit to model the Rossiter-McLaughlin effect. The amplitude of this radial velocity deviation is only 10 m s^{-1}, consistent with the small ratio of the planet to star radius. A self consistent model that includes Doppler and

photometric data shows that the equatorial plane of this star is aligned with the orbital plane to within a few degrees (Wolf et al. 2005).

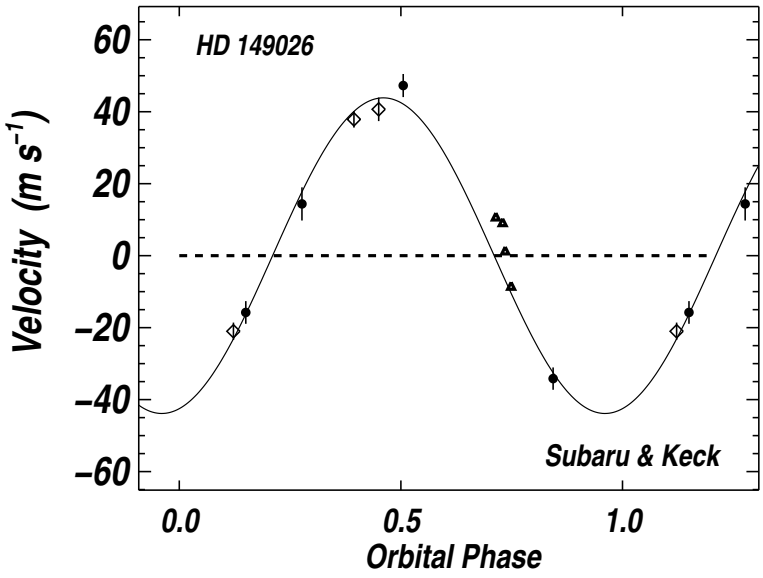

Figure 4. *Phased radial velocities for HD 149026 from Subaru (filled circles) and Keck (open diamonds). The triangles represent RV measurements made at Keck during transit, and exhibit the Rossiter-McLaughlin effect With an orbital period of 2.8766 day, velocity amplitude of 43.3 m s^{-1} and stellar mass of 1.3 $M_\odot$, the implied planet mass is $M \sin i$ = 0.36 $M_{\rm Jup}$ and the orbital radius is 0.042 AU.*

Photometric follow-up of this system by Greg Henry, using the automatic photometric telescopes at Fairborn Observatory demonstrated a repeated 3 millimag decrement in stellar brightness within 1 hour of the Doppler-predicted transit times. The transit duration and model fit ruled out grazing eclipsing binaries and provided an orbital inclination of at least 84 degrees. Subsequent photometry by Charbonneau et al. (2005b) confirms these photometric results.

The stellar radius is a critical parameter since only the ratio of the planet radius to the stellar radius is well-determined by the transit depth. Based on the stellar luminosity and effective temperature, we derived a stellar radius of 1.45 $R_\odot$. Together with the shallow photometric transit data, the stellar radius implies a planet radius of only 0.72 $R_{\rm Jup}$. Modeling of this system by Peter Bodenheimer suggests a

stunningly large core mass. Depending on the assumed central density (either ρ_c=5.5 g cm^{-3} or ρ_c=10 g cm^{-3}) the core of HD 149026 is between 78 and 67 $M_\oplus$ respectively. This core is in striking contrast to Jupiter in our own solar system (Figure 5).

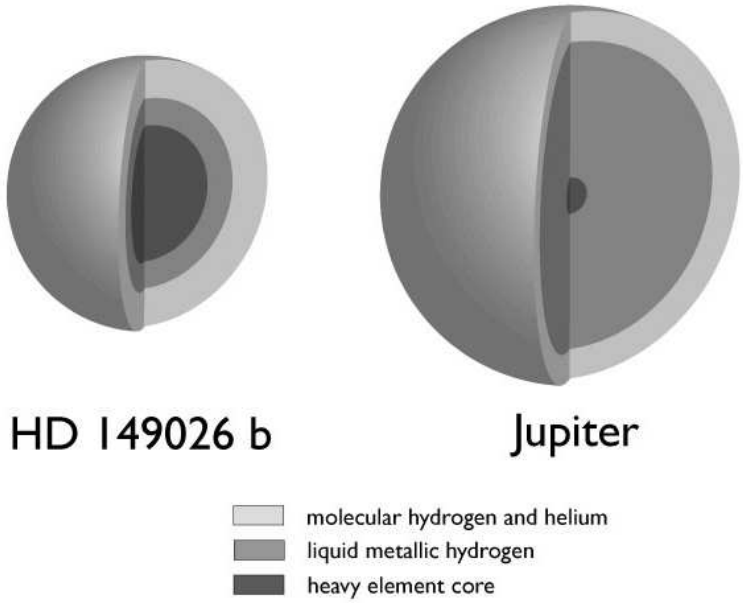

Figure 5. *A comparison of the interior structure of HD 149026b and Jupiter. The sizable model core underscores the diversity of interior structure that seems to exist in gas giant planets. This diagram by G. Laughlin, is based on models of Peter Bodenheimer.*

4. Conclusions

Because brightness matters for radial velocity precision, magnitude limits in our selection process may introduce a Malmquist bias that favors the inclusion of intrinsically more luminous subgiants in the N2K database. While the transit probabilities go up by a few percent for stars with larger radii, the transit depths decrease, making high precision photometry very important.

It is notable that three of the four planets found from the N2K survey in the past year have masses comparable to Saturn. Even shallower transit depths would be expected for Saturn-mass planets. HD 88133 has a radius of 1.93 $R_\odot$ and a planet mass, $M \sin i$ = 0.25

$M_{\rm Jup}$; HD 149143 has a radius of 1.49 $R_\odot$ and a planet mass of 1.32 $M_{\rm Jup}$; HD 109749 has a stellar radius of 1.24 $R_\odot$ and a planet mass of 0.27 $M_{\rm Jup}$, and HD 149026 has a radius of 1.45 $R_\odot$ and a planet mass of 0.36 $M_{\rm Jup}$.

HD 149026b was recently observed to transit its host star with a transit depth of only 3 millimags. The small photometric depth of the transit of the planet underscores its most novel property, a massive $\sim 70\ M_\oplus$ core. The apparent presence of this large core has a number of potentially interesting ramifications for the theory of planet formation. Perhaps most important, it would be difficult to form this giant planet by the gravitational instability mechanism (Boss 2004). At the same time, conventional core accretion models would predict runaway gas accretion for such a massive core, so this system also presents challenges for core accretion models. The detection of additional transiting planets around bright stars should add considerably to our understanding of the formation and structure of extrasolar planets.

There were two necessary components for the 3 millimag transit detection of HD 149026. First, the initial Doppler reconnaissance at Subaru and Keck detected the low-mass, short-period planet and provided an accurate ephemeris prediction. Second, the robotic telescopes at Fairborn Observatory were available to obtain baseline photometry and to carry out millimag-precision photometric observations at the predicted transit times. This approach, combining a quick-look, Doppler survey with targeted high-precision photometry has turned out to be an efficient way to detect transiting planets around bright stars.

Acknowledgements. We acknowledge the contributions of all members of the N2K consortium. We acknowledge travel support for this conference from NASA grant (to DAF).

References

Alonso, R., Brown, T. M., Torres, G., *et al.*, 2004, ApJ, 613, L153

Ammons, M., Robinson, S. E., Straeder, J., Laughlin, G., & Fischer, D. 2005, ApJ, in press

Bouchy, F., Udry, S., Mayor, M., *et al.*, 2005, A&A, 444, L15

Boss, A. P. 2004, ApJ, 610, 456

Charbonneau, D., Allen, L. E., Megeath, S. T., *et al.*, 2005a, ApJ, 626, 523

Charbonneau, D., Winn, J. N., Latham, D. W., *et al.*, 2005b, ApJ (submitted)

Charbonneau, D., Brown, T. M., Noyes, R. W., & Gilliland, R. L. 2002, ApJ, 568, 377

Charbonneau, D., Brown, T. M., Latham, D. W., & Mayor, M. 2000, ApJ, 529, L49

DeMarque, P., Woo, J. H., Kim, Y. C., & Yi, S. K. 2004, ApJS, 155, 667

Deming, D., Brown, T. M., Charbonneau, D., Harrington, J., & Richardson, L. J. 2005, ApJ, 622, 1149

Fischer, D. A., & Valenti, J. A. 2005, ApJ, 622, 1102

Fischer, D. A., *et al.*, 2005a, ApJ, 620, 481

Fischer, D. A., *et al.*, 2005b, ApJ, in press

Fortney, J. J., Marley, M. S., Lodders, K., Saumon, D., & Freedman, R. 2005, ApJL, 627, 69

Gonzalez, G. 1998, A&A, 334, 221

Henry, G. W., Marcy, G. W., Butler, R. P., & Vogt, S. S. 2000a, ApJ, 529,L41

Mayor, M., & Queloz, D. 1995, Nature, 378, 355

Santos, N. C., Israelian, G., & Mayor, M. 2001. A&A, 373, 1029

Santos, N. C., Israelian, G., Mayor, M., *et al.*, 2005, A&A, 437, 1127

Sato, B., Fischer, D., Henry, G., *et al.*, 2005, in press

Valenti, J. A. & Fischer, D. A. 2005, ApJ, in press

Vidal-Madjar, A., Désert, J.-M., Lecavelier des Etangs, A., *et al.*, 2004, ApJL, 604, 69

Wolf, A., *et al.*, 2005, in preparation

Tenth anniversary of 51 Peg-b : Status of and prospects for hot Jupiter studies
Proceedings of Haute Provence Observatory Colloquium (22-25 August 2005)
Edited by L. Arnold, F. Bouchy, and C. Moutou

Statistics of masses and orbital parameters of extrasolar planets using continuous wavelet transforms

R.V. Baluyev[1]

[1]*Saint Petersburg State University (Sobolev Astronomical Institute), 198504 Universitetskij pr. 28, Petrodvoretz, Saint Petersburg, Russia [m01brv@star.math.spbu.ru]*

Abstract. At the present time (September, 2005) more than 150 exoplanetary candidate companions to solar-type stars are known. Such data amount is hardly sufficient for statistical researches. The classical statistical technique (histograms, cumulative distribution, etc.) provides low precision when using for comparison different distribution function values (for example, testing the distribution on structures like heterogeneities). The reason lies in a fact that a way to represent distribution function as a collection of its values is not suitable for such situation. In the present work an approach based on an effective technique of data analysis using wavelet transformations is built. General features of the wavelet analysis of statistical data are described, the practically important statistical tests are constructed. A number of univariate distributions of basic parameters (exoplanetary minimum masses, orbital periods, semi-major axes and eccentricities) are examined. The possible prospects for this technique development are discussed.

1. Introduction

A number of the candidate planetary companions to solar-like stars have exceeded $N = 160$ (Schneider 2005). Such sample size provides a precision at the level $1/\sqrt{N} \approx 0.08$ (note, that this is a rough value for *relative error* of some parameter estimation, for instance, and never associated with any *probabilities* involved in statistical tests). Such precision level indicates that the current sample size is hardly enough to derive reliable statistical results. The other implication is that one

should put very strong requirements on the used data analysis technique efficiency to preserve this not very high precision.

Let us adopt a non-parametric situation when one wishes to extract some information from distribution in question without imposing any model to the data. This part of statistics is not so close to perfect as an opposite parametric one. The reason seems being from a fact that it is difficult to state clearly in general situation the desirable kind of information to be derived. This implies non-universality of non-parametric methods.

Nevertheless, in the present work an attempt to state such strict and simultaneously maximally general requirement was made. Namely, the distribution information is assumed containing in specific distribution function structures, determinable by differences between neighbor values in the whole sequence of this function values.

The usual classic techniques (histogram coupled with Pearson χ^2-test, empirical cumulative distribution with Kolmogorov goodness-of-fit test, for example) are not suitable for revealing local features possessing differential property, because they are aimed to test the single distribution function value neglecting the environmental ones. Moreover, a way to represent distribution functions as a sequence of their values can not be suitable for the stated goal. The better way of function representation should consider their derivatives.

2. Application of continuous wavelet transforms in statistics

Let us introduce a real-value function $\Psi(s)$ of the real argument s such that it may be used for local smoothing, i.e. it is well concentrated near $s = 0$, its Fourier image

$$\widehat{\Psi}(\omega) = \int_{-\infty}^{+\infty} \Psi(s) e^{i\omega s} ds$$

is also well concentrated near $\omega = 0$ and, in addition, $\widehat{\Psi}(0) = 1$. Thus one may construct a family of differential wavelets

$$\Psi_j(s) = (-1)^j \frac{d^j \Psi}{ds^j}(s), \quad \widehat{\Psi}_j(\omega) = (i\omega)^j \widehat{\Psi}(\omega), \quad j \geq 1 \tag{1}$$

having $\widehat{\Psi}_j(0) = 0$ and satisfying admissibility condition (see Section 4.).

Definition 1. Let j^{th} order Ψ-derivative wavelet transform (WT) of a real-value function $f(t)$ of a real argument t be

$$W_{\Psi,j}[f](a,b) = \int_{-\infty}^{+\infty} \Psi_j \left(\frac{t-b}{a} \right) f(t) \frac{dt}{a^{j+1}}. \tag{2}$$

Note that the normalization used here slightly differs (for the further comfortability reason) from standard one used by Daubechies (1992).
Definition 2. Let us define j^{th} order Ψ-derivative WT of a real random variable τ having probability density function (PDF) $f(t)$ as

$$W^{[\tau]}_{\Psi,j}(a,b) = W_{\Psi,j}[f](a,b). \tag{3}$$

Note, that $W^{[\tau]}_{\Psi,j}(a,b)$ represents mathematical expectation of the function $\Phi_{a,b}(\tau) = a^{-j-1}\Psi((\tau-b)/a)$. One may easily derive that

$$W^{[\tau]}_{\Psi,j}(a,b) = W_{\Psi,0}[f^{(j)}](a,b). \tag{4}$$

This means that j^{th} WT of a random variable coincides with a smoothed j^{th} derivative of this variable PDF. This property becomes very useful in statistical data analysis. It is necessary to smooth data to reduce statistical noise. It is not rational to smooth the function in question itself, because such smoothing reduces real small-scale structures. Such structures are much more contrast in derivatives of the distribution function and may be saved in it. For example, one should use the first Gaussian wavelet for revealing such structures as sharp cutoffs (when the first PDF derivative is large) and the second one ("Mexican hat") to test PDF on peaks and gaps (when the curvature of PDF graph is large).

The choice of base smoothing function $\Psi(s)$ is not an easy question. This arbitrary is not a property of wavelet transform technique only and seems to be rather general. So, the histogram is based on a rectangular filter, but we are not limited in using any other. We adopt for practical applications a Gaussian smoothing filter due to its equal concentration both in space and frequency and its mathematical simplicity. This base filter generates a family of Gaussian wavelets $\psi_j(s)$ and Gaussian WT. We will denote the latter as $W_j(a,b)$ (omitting base filter mark). The mark of either random variable (or PDF) and even wavelet order will be often omitted too, what will not lead to misunderstandings.

3. Statistical tests with wavelets

The unbiased estimation of the value $W(a,b) = \mathbf{E}\Phi_{a,b}(\tau)$ based on a random sample $\mathcal{T} = \{t_i\}_{i=1}^N$ is a mean

$$\widetilde{W}(a,b) = \frac{1}{N}\sum_{i=1}^{N}\Phi_{a,b}(t_i). \tag{5}$$

The next step is to construct goodness-of-fit tests. The two limiting situations differing by accessibility of prior information may take place. In order to follow Vityazev (2001) they will be referred as H_1 and H_2.

H_1. Position and scale (a, b) of a possible structure are unknown *a priori*. The question is "Are *all* differences between a given model $W(a, b)$ and estimation $\widetilde{W}(a, b)$ explainable by statistical noise only?". That is a more general situation than the next one.

H_2. Values (a, b) of a possible structure are known *a priori* (from theory, for example). One wishes to test "Is *the only one* difference $\widetilde{W} - W$ significant or not?".

A test for H_2 situation may be easily constructed. The value $\widetilde{W}$ asymptotically ($N \to \infty$, the conditions of central limit theorem are satisfied if wavelets being used are localized well enough) follows normal distribution with a mean W and standard deviation $\mathbf{D}\widetilde{W} = \mathbf{D}\Phi/N$. The latter's unbiased estimation is

$$D = \frac{1}{N(N-1)} \sum_{i=1}^{N} (\Phi(t_i) - W)^2.$$

The quotient $g = (\widetilde{W} - W)/\sqrt{D}$ is a statistics of the test. Its asymptotic ($N \to \infty$) distribution is a standard normal distribution $\mathcal{N}(0, 1)$.

Not the same is in H_1 situation. The probability to make false alarm while testing many values $\widetilde{W}(a, b) - W(a, b)$ (infinitely many!) is much higher than while testing the only one difference. In order to reach linear invariance of the test the values of random function $Y(a, b) = a^{j+1}(\widetilde{W}(a, b) - W(a, b))$ should be used (due to adimensionality of Y). In terms of cumulative τ distributions (model F and empirical $\widetilde{F}$ ones)

$$Y(a, b) = \int_{-\infty}^{+\infty} \frac{d}{dt} \left[\Psi_j \left(\frac{t - b}{a} \right) \right] \left(F(t) - \widetilde{F}(t) \right) dt.$$

In term of Kolmogorov statistics $\Delta = \max_t(\widetilde{F}(t) - F(t))$ one gets for statistics $\zeta = \max_{a,b} |Y(a, b)|$ an inequality $\zeta \leq V_j \Delta$, where V_j being a total variation of j^{th} wavelet. Thus $\Pr\{\zeta > z\} \leq K(z/V_j)$, where $K(z) \sim 2e^{-2Nz^2}$ being Kolmogorov limiting distribution function. But this estimation is far from an actual ζ distribution (either due to badness of the estimation used or due to low power of Kolmogorov test). It seems to be difficult to find significantly preciser upper estimation analytically by elementary techniques, what makes us to use Monte-Carlo simulations. Figure 1 shows results of these simulations for Gaussian wavelets and for a number of continuous cumulative distributions of τ (the values of their parameters plays no role due to linear invariance of

the test, except the case of the two Gaussian peaks when on the main Gaussian with a weight 0.7 and dispersion σ a secondary peak with a weight 0.3 and dispersion 0.5σ was placed with a shift of 1.0σ). It may be clearly seen that the distribution of ζ depends weakly on distribution of τ. Moreover, the former one may be well limited by Gumbel distribution functions of the kind $G(A\sqrt{N}, B, z) = \exp\left(-\exp\left(-Az\sqrt{N} + B\right)\right)$ where two parameters A, B depend on wavelet being used.

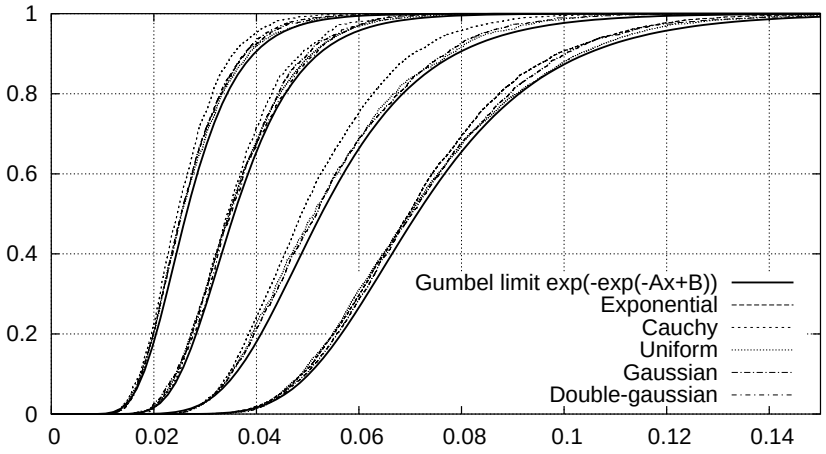

Figure 1. *Simulation results for cumulative distribution of ζ statistics. The count of treats varies from 1000 to 5000. The curves are plotted for (N, j) values of (100,1), (100,2), (25,1), (25,2), from left to right.*

4. The inverse wavelet transform and restoring the probability density function

The inverse WT (IWT) in terms being used looks like

$$\begin{aligned} f(t) &= C_{\Psi,j}^{-1} \int_{-\infty}^{+\infty} \int_{-\infty}^{+\infty} W_{\Psi,j}[f](a,b) \Psi_j \left(\frac{t-b}{a}\right) a^{j-2} da db, \\ C_{\Psi,j} &= \int_{-\infty}^{+\infty} \left|\widehat{\Psi}_j(\omega)\right|^2 \frac{d\omega}{|\omega|}, \end{aligned} \tag{6}$$

if constant $C_{\Psi,j}$ is finite (note, that $C_j = (j-1)!$ for Gaussian wavelets). The latter condition $C_{\Psi,j} < +\infty$ is so-called "admissibility condition". One may use expression (6) to restore probability density $f(t)$ by cleared from statistical noise WT using tests described above. The only difficulty is that an arbitrary function $W(a, b)$ (like a cleared WT) is *not*,

in general case, a WT of any function. After formal application of the IWT, the WT of the found in such way function $f(t)$ differs from initial $W(a,b)$, but is close to it. The solution is to carry out these iterations until the difference becomes non-significant (for H_1 situation until $\zeta \leq z$ where z being a confidence threshold). The output function $f(t)$ is a probability density function cleared from non-significant differential structures. This algorithm is related to a well known "CLEAN" one being used in time series analysis and radioastronomy.

5. Application to statistics of extrasolar planets

The wavelet technique was applied to the known sample of 168 exoplanetary candidates (Schneider 2005). The above algorithm of univariate PDF cleaning was applied to a number of important parameters: exoplanetary orbital periods, semi-major axes, minimum masses, eccentricities. Volume limitation does not allow to describe all of them and make us to consider the first and, partly the second ones only.

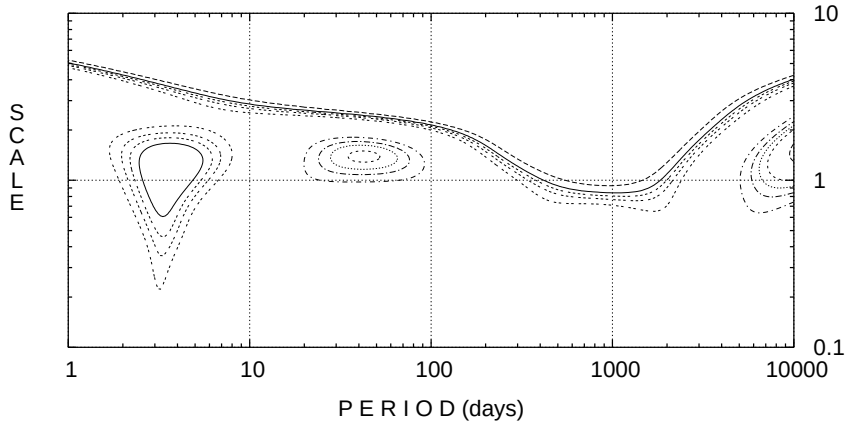

Figure 2. *Wavelet transform of exoplanetary orbital period logarithms. The "Mexican hat" wavelet ($j = 2$) used. Contours of equal false alarm probability for values* 0.50, 0.20, 0.10, 0.05 *and* 0.01 *calculated for* H_1 *situation framework are shown.*

Figures 2 and 3 show contours of false alarm probability (fap) of WT of period logarithms ($j = 2$), calculated for situations H_1 and H_2, respectively. One may see hot Jupiters peak (periods of $2-6$ days) having $fap \approx 0.02$, followed by "period valley" with $fap \approx 0.04$ (periods less than 100 days). These structures are significant in H_1 situation.

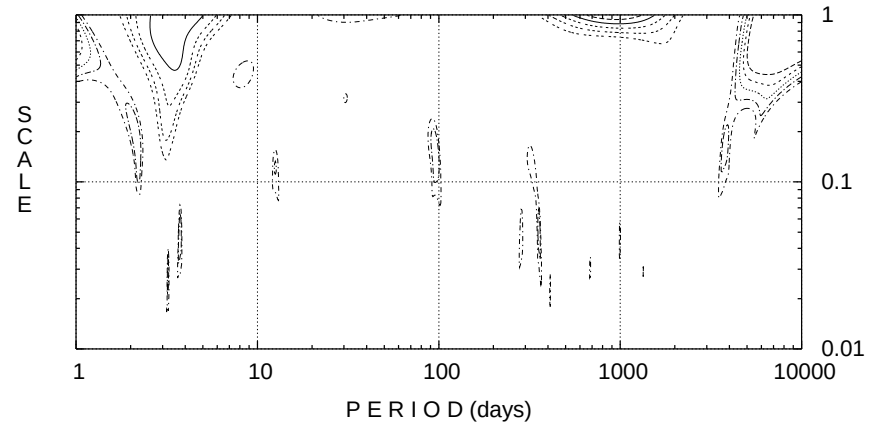

Figure 3. *Wavelet transform of exoplanetary orbital period logarithms. The same as Figure 2, except H_2 situation applied. Significance levels are 2.5σ, 3.0σ, 3.5σ, 4.0σ and 4.5σ.*

The H_2 situation figure shows a small-scale structure centered very precisely at one-year period. This "absorption line" represents an evidence of an alias effect, when periodic gaps in observational time moments make it difficult to derive resonant periodicity from such data. The semi-major axes distribution (not shown) looks very similar to period distribution, except corresponding significances are slightly smaller in this case (probably, due to errors in stellar masses values). The alias effect disappears in semi-major axes distribution (due to a scattering of stellar masses near solar). The Figure 4 shows restored PDF plots for fap values in the range $0.01 - 0.50$. It may be stated that although the hot Jupiters peak seems to be reliably significant, its numerical parameters are not derivable reliably with a current sample size. This peak rapidly decreases while required confidence probability increases from 50% to 95% and is not presented in PDF cleared at the level of 99% confedence. It may be estimated that the whole hot Jupiter peak (assuming its size as it is seemed from the present sample) would be significant at the level of 99% with a sample of a size six time larger then the current, i.e. when $N \approx 1000$. The bright example of statistical noise was possessed recently by exoplanetary sample: before the conference proceedings the fap of hot Jupiter peak was only 8%. The further increase of exoplanetary candidates number during a fortnight produced the results stated above. Really six new points added to 162 can judge adequately?

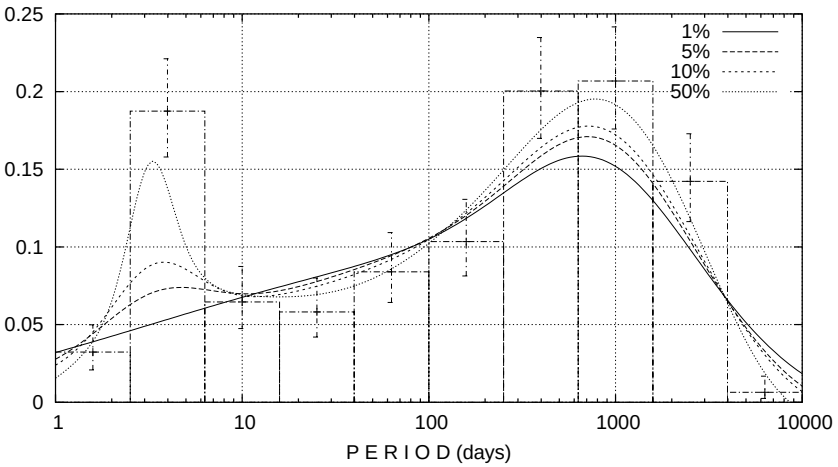

Figure 4. *Restored exoplanetary orbital periods PDF plotted for a number of confidence levels with a normalized periods histogram. The same conditions as of Figure 2.*

6. Conclusions and prospects

The described technique of PDF representation by its decomposition in differential wavelets showed its high efficiency. The possible prospect for this technique development is to generalize it to multi-dimensional distributions. The other one represents a possible way to account observational selection which plays a very high role in statistics of extrasolar planets. The selection effects usually may be represented as an integral transforms subjecting the PDF in question. One may transform an analyzing wavelet kernel so that the output transformation will be free (at least partially) from selection distortion.

Acknowledgements. The author would thank Dr. B.R. Mushailov and Dr. K.V. Kholshevnikov for fruitful discussions on the subject of this paper.

References

Schneider, J. September 2005, *The Extrasolar Planets Encyclopaedia*, web site at http://www.obspm.fr/planets.

Daubechies, I. 1992, *Ten Lectures on Wavelets*, Society for Industrial and Applied Mathematics, Philadelphia.

Vityazev, V.V. 2001, *Spectral Analysis of Unevenly Spaced Time Series*, Saint Petersburg University Press, Saint Petersburg.

Tenth anniversary of 51 Peg-b : Status of and prospects for hot Jupiter studies
Proceedings of Haute Provence Observatory Colloquium (22-25 August 2005)
Edited by L. Arnold, F. Bouchy, and C. Moutou

Any hot-Jupiter around M dwarfs ?

X. Bonfils[1,2], X. Delfosse[2], S. Udry[1], T. Forveille[3,2], and D. Naef[4]

[1] *Observatoire de Genève, 51 ch. des maillettes, CH-1290 Switzerland [Xavier.Bonfils@obs.unige.ch]*

[2] *Laboratoire d'Astrophysique, Observatoire de Grenoble, BP-53, F-38041 Grenoble, Cédex 9, France*

[3] *Canada-France-Hawaii Telescope Corporation, 65-1238 Mamalahoa Highway, Kamuela, HI96743, Hawaii, USA*

[4] *European Southern Observatory, Alonso de Cordova 3107, Casilla 19001 Santiago 19, Chile*

Abstract. While over 160 planets have been found to orbit F, G and K stars, only five have been found around M dwarfs. In spite of their small number, the planets identified around very-low-mass stars exhibit some interesting statistical properties. In particular, they include no hot-Jupiter and very few Jupiter-mass planets at any period. A different frequency of Jupiter-mass planets between sun-like stars and M dwarfs may point toward a stellar mass dependency in planet formation processes. Our recent work on M-dwarf metallicity suggests however that they might have lower abundances of heavy elements than earlier-type stars. Given the well established overabundance of planets around metal-rich stars, one needs to verify whether metallicity alone can explain the statistical properties of M-dwarf planets. We use simulations to investigate how detection biases affect the apparent frequency of planets orbiting M dwarfs, and to check how the lower mean metallicity of M dwarfs would affect their planet population if the planet-metallicity correlation found for sun-like stars applies to them as well.

1. Introduction

The reasons for hunting for planets around M dwarfs are many, but the main one is that comparison of their properties with those around solar-type stars probes the dependence of planet formation acting on stellar mass. M dwarfs are also the dominant population of our Galaxy (by both mass and number, Chabrier & Baraffe 2000), so looking at them is needed for a global view of the planet population of our Galaxy. Finally, quiet M dwarfs are stable to 1-m s^{-1} precision (Bonfils et al. 2005a) and their habitable zone is much closer to the star, making them prime targets in searches for habitable telluric planets.

2. Status

Our group and several others use radial-velocity monitoring to search for planets around M dwarfs (e.g. Bonfils et al. 2004; Endl et al. 2003; Kuerster et al. 2003; Wright et al. 2004). The target samples have partial overlap, but altogether comprise over 200 M dwarfs.

These efforts have up to now led to the discovery of 3 planetary systems around M dwarfs. Gl 876, was the first M dwarf found orbited by a planet (Delfosse et al. 1998; Marcy et al. 1998) and its planet count currently stands at 3. Two have Jupiter-like masses (Marcy et al. 2001), and the third one belongs to the Neptune-like mass domain of Neptune and is the lightest found so far (Rivera et al. 2005). This system, hierarchically organized and resonant, remains challenging for planetary formation theory. The two other M dwarfs with planets, Gl 436 (Butler 2004) and Gl 581 (Bonfils et al. 2005a), both have single Neptune-mass companions in short-period orbits.

These detections contrast with the characteristics of the planet population of F, G and K stars: $f_p \simeq 1\%$ of these sun-like stars are orbited by hot Jupiters (i.e. planets with 0.5 $M_{Jup} < M_p < 10$ M_{Jup} and 1 day $< P <$ 5 days), and $f_p \simeq 4-5\%$ by planets with 1 $M_{Jup} < M_p < 10$ M_{Jup} and $P <$ 1500 days (Zucker & Mazeh 2001; Tabachnik & Tremaine 2002; Lineweaver & Grether 2003; Naef et al. 2005). Our goal here is to evaluate through simulations (Sect. 4.) how much of this difference is intrinsic, rather than due to observational biases. We also consider the influence of metallicity in Sect. 5.

3. Samples

Our search for planets around M dwarfs is based on two radial-velocity programs. In the northern hemisphere we have used ELODIE (Baranne et al. 1996) since 1996 to observe a volume limited sample (d<9.25 pc)

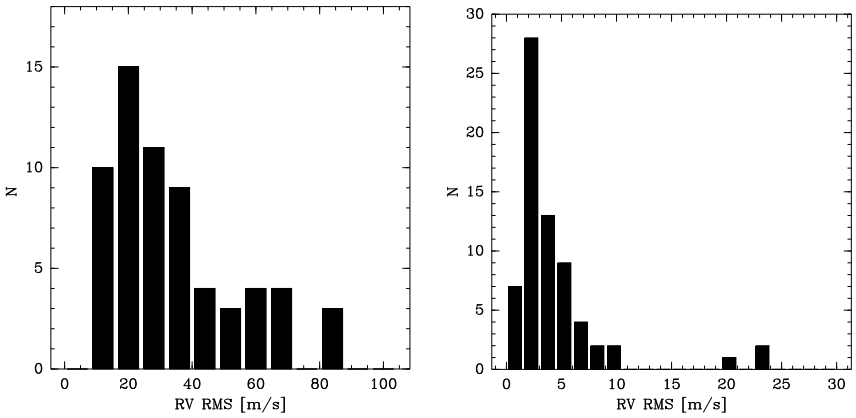

Figure 1. *Distribution of radial-velocity dispersions for the well observed stars in our ELODIE (left panel) and HARPS (right panel) programs. These dispersions include the photon noise, the radial-velocity "jitter" due to stellar activity, as well as variations due to undetected planetary companions.*

of ∼100 M dwarfs with a precision close to the photon noise. Depending on stellar brightness, this ranges from 10 to 70 $\mathrm{m\,s^{-1}}$ (Fig. 1). In the southern hemisphere we use HARPS (Pepe et al. 2004) and observe a volume limited sample (d<11 pc) of ∼110 M dwarfs.

In order to investigate the statistical properties of planets around M dwarfs we evaluate the completeness of the planet detection in our observing programs (Sect. 4.). Many of the observed stars display high radial-velocity (RV) dispersion for reasons other than a planet: a stellar binary companion (close visual or spectroscopic), magnetic activity, fast rotation, or large measurement errors for the fainter stars. We therefore restrict our analysis to subsamples that only retain stars without a well identified cause of RV variation. These subsamples are thus cleaned from binaries and fast rotators ($v \sin i \geq 6.5$ $\mathrm{km\,s^{-1}}$), and reject the faintest stars ($m_V > 14$). We also remove one star with a high RV dispersion which a bisector analysis shows is due to activity, and the 3 stars with known planets. Finally, the HARPS program is too recent for all stars to have enough measurements to measure a meaningful dispersion, and we only retain the 68 stars with at least 3 measurements. To obtain reasonable statistics we perform the analysis on a merged sample of the ELODIE and HARPS subsamples, which contains 112 M dwarfs.

4. Simulations

We explore the sensitivity of our measurements to planets of varied characteristics to evaluate our detection completeness.

4.1 Method

We build a $M_p \sin i$ versus P grid and for each grid point we simulate 1000 orbits. For that we randomly pick both the remaining orbital parameters ($T0$, e, ω), and the parameters of one star from the sample (characterized by its mass, the calendar of its observations, and its radial velocities and associated errors). Initial tests showed that eccentricity e has little influence, and for production runs we fixed it to zero. ω then becomes irrelevant, leaving only $T0$ and the characteristics of a star to be chosen randomly. The 100 $\times$ 500 grid is evenly spaced in a logarithmic scale and fine enough to efficiently sample the typical observation spacing (e.g. around 1 day, 6 months and 1 years). It spans periods from 1 to 7000 days and projected masses from 1 $M_\oplus$ to 13 M_{Jup}.

For each simulated orbit we calculate the radial-velocity variation induced by the virtual planet at the actual dates of observations, and add the poissonian noise expected from photon noise to each of the individual measurements. We then compare the dispersion of these *simulated* radial velocities, RMS_{SIM}, with that of the *observed* ones, RMS_{OBS}. If $RMS_{SIM} > RMS_{OBS}$ the simulated planet does not exist. *A contrario*, if $RMS_{SIM} \leq RMS_{OBS}$, our observation cannot tell whether such a planet exists or not. This comparison is done for each of the 1000 realizations for each grid point. For stars observed with both instruments the simulated planet is considered not to exist when at least one of the RMS_{OBS} is smaller than RMS_{SIM}. This finally yields a frequency of planets our program can not reject for each chosen mass and period, i.e. it yields a minimum frequency of M dwarfs that do not have planets.

4.2 Results

We first focus on hot Jupiters, for which we use the joint ELODIE+HARPS sample. Hot Jupiters around Sun-like stars are concentrated in the domain 0.5 $M_{Jup} < M_p \sin i < 2$ M_{Jup} and 1 day < P < 5 days. They give large velocity amplitudes, and when averaging over this box we find that virtually 100 % of the simulated orbits would be rejected as actual planets on our sample. The ELODIE+HARPS sample contains 112 stars, to which we add back the 2 stars with planets which were initially set aside and which contain no hot Jupiter. Taking into account the statistical uncertainty from the finite size of the sam-

ple, this sets upper limits to the frequency f of hot Jupiter orbiting M dwarfs to $f < 1$ % at a 68.3 % confidence level and to $f < 5$ % at a 99.7 % confidence level. The lack of hot Jupiters around M dwarfs is therefore suggestive, but from our observations alone still of modest significance.

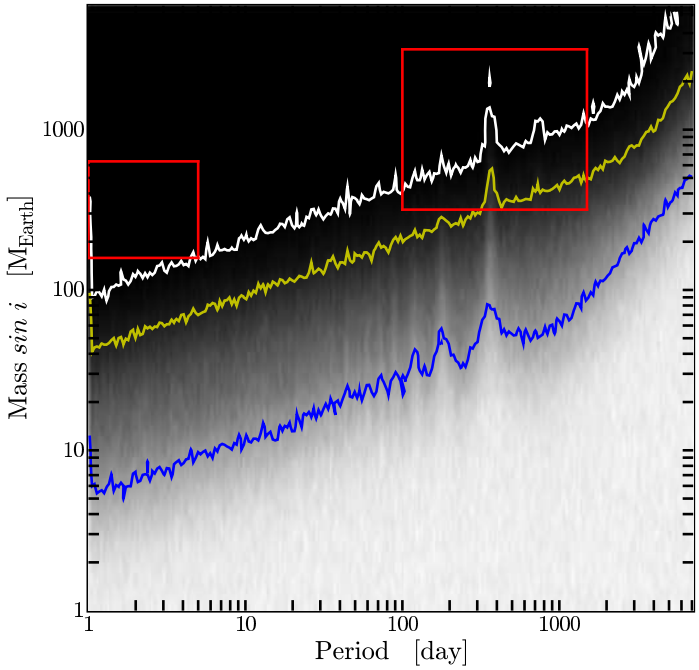

Figure 2. *Non detection statistic applied to the merged ELODIE+HARPS sample. Lines are iso-frequency for non-detection (1, 10 and 50 %, from top to bottom). The boxes delineate the regions where we compute upper limits to the frequency of planets for hot Jupiters and long-period Jupiter-mass planets.*

Longer periods Jupiter-mass planets of sun-like stars ($P <$ 1500 days, 1 $M_{Jup} < M_p \sin i < 10\ M_{Jup}$) are concentrated in region with periods between 100 and 1500 days which they fill homogeneously. Using our large sample we thus compute an average frequency in this region. Our simulation shows that $\sim$ 98.8% of the simulated planets can be rejected. A more complex use of our simulator (described in a forthcoming paper) permits to disentangle the non-detections due to time sampling ($\sim$ 0.3%) from the ones due to a real RMS excess ($\sim$ 0.9%).

While firsts reflect the incompleteness of our survey, seconds represent either activity or undetected companions (however not necessarily in the present mass-period region). To the 112 stars considered we add *a posteriori* the 2 planet-host stars, one of which (Gl 876) hosts planets in the Jupiter-mass range and with periods below 1500 days. To derive a confidence interval we may consider either the only real detection either assume there is $\sim 0.9\% \times 112 = 1$ more planet host. We made the conservative choice to derive the lower boundary of the confidence interval assuming only one detection and the upper boundary assuming 2 detections. Hence the frequency f of Jupiter-mass planets orbiting M dwarfs range between $0.6\ \% < f < 4\ \%$ at the 68.3 % confidence level and between $0.05\ \% < f < 9\ \%$ at the 99.7 % confidence level.

In both period domains the frequency of Jupiter-mass planets thus appears low, but the difference from sun-like stars still has relatively low statistical significance.

5. Effect of metallicity

One remarkable statistical property of solar-type planet-host stars, identified soon after the first discoveries, was that exoplanets are mostly found around metal-rich stars (Gonzalez 1997, 1998). Santos et al. (2001, 2003) compared samples of stars *with* and *without* planets extracted from the same planet-search program and analyzed them identically. They confirmed, free of any relative bias between these two samples, that planet-host stars are statistically much more metal rich than stars without planet.

This correlation is not (yet) established for stars with a Neptune-mass planet, or for planets around M dwarfs. The metallicity distribution of the FGK stars known to host a Neptune-mass planets is rather flat, though the overall number is small (4). The observations which found these planets on the other hand were were often a follow-up of stars with previously known Jupiter-mass planets, a fact which should have biased this sample toward high metallicities (the giant planet detection favors a a metal-rich hosts). We also estimated the metallicity of the 3 M dwarfs that host known planets and found that they are approximately solar (Bonfils et al. 2005b).

We recently measured the difference between the mean metallicity of M dwarfs and sun-like stars (Bonfils et al. 2005b), and found M dwarfs to be metal-poor by 0.06 dex. The difference is still of modest significance (2.6 σ), but is in the direction expected from the history of the Galaxy: some of the oldest (metal poor) sun-like stars have left the main sequence, while all M dwarfs are still here for us to see. If planet formation has the sensitivity to metallicity for sun-like stars and M

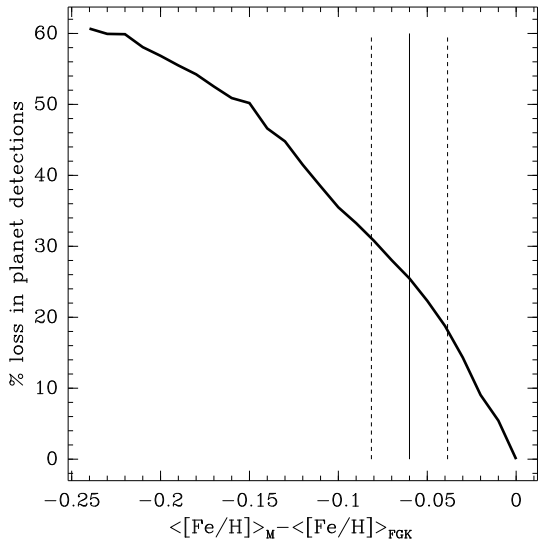

Figure 3. *Drop in planet detections (in %) as a function of the mean metallicity difference between sun-like stars and M dwarfs. It assumes the planet-metallicity correlation does not depend on the star's mass. The vertical thin line indicates the mean metallicity we found for M dwarfs. The dashed lines correspond to its 1 σ uncertainty.*

dwarfs, such a difference will decreases its efficiency around M-dwarfs. To quantify this expected deficit, we use the metallicity distribution of the 1000 single stars of the CORALIE planet search (Udry et al. 2000), shifts this distribution by 0 to -0.25 dex (with 0.01 dex steps), and evaluate how this affects the expected number of planets for the metallicity dependence of the planet frequency proposed by Santos et al. (2004, Fig. 6). Fig. 3 illustrates the resulting planetary deficit as a function of the metallicity difference, and shows that the observed metallicity difference (0.06 dex) would result in a 20-30% deficit around M dwarfs. Metallicity is therefore not the main explanation for the apparent larger observed deficit.

6. Conclusions & Prospects

We have presented the most precise estimate to date for the frequency of planet around M dwarfs. It points toward a low frequency of Jupiter-mass planets, though for now with relatively modest statistical significance due to our still small (O(100)) sample. If the planet-metallicity correlation applies to Jupiter-mass planets orbiting M dwarfs, the lower

mean metallicity of M dwarfs could explain some of this difference, but most likely not all of it.

A striking characteristic emerging from M dwarfs observations is the large fraction of Neptune-mass close-in planets. Additional detections will make the statistic more robust, but they already seem more common around M dwarfs, as predicted by theory (Laughlin, Adams & Bodenheimer 2004; Ida & Lin 2005).

Acknowledgements. We deeply thank the many collaborators who have contributed to the observations for our ELODIE and HARPS observing programs.

References

Baranne, A., Queloz, D., Mayor, M., *et al.*, 1996, A&A, 119, 373

Bonfils, X., Delfosse, X., Udry, S., *et al.*, 2004, in *Extrasolar Planets: Today and Tomorrow*, ASP Conference Proceedings, 321, 1001

Bonfils, X., Delfosse, X., Udry, S., *et al.*, 2005, A&A, 442, 635

Bonfils, X., Forveille, T., Delfosse, X., *et al.*, 2005, A&A preprint doi http://dx.doi.org/10.1051/200500193

Chabrier, G. & Baraffe, I. 2000, ARA&A, 38, 337

Delfosse, X., Forveille, T., Mayor, M., *et al.*, 1998, A&A, 338L, 67

Endl, M., Cochran, W. D., Tull, R. G. & MacQueen, P. J. 2003, AJ, 126, 3099

Gonzalez, G. 1997, MNRAS, 285, 403

Gonzalez, G. 1998, A&A, 334, 221

Ida S. & Lin D. N. C. 2005, ApJ, 626, 1045

Kürster, M., Endl, M., Rouesnel, F., *et al.*, 2003, A&A, 403, 1077

Laughlin G., Adams P., & Bodenheimer F.C. 2004, ApJ, 612L, 73

Lineweaver, C. H. & Grether, D. 2003, ApJ, 598, 1350

Marcy, G. W., Butler, R. P., Vogt, S. S., *et al.*, 1998, ApJ, 505L, 147

Marcy, G. W., Butler, R. P., Fischer, D., *et al.*, 2001, ApJ, 556, 296

Naef, D., Mayor, M., Beuzit, J.-L., *et al.*, 2005, Proceedings of the 13th Cambridge Workshop on Cool Stars, Stellar Systems and the Sun, ESA SP-560, p. 833.

Pepe, F., Mayor, M., Queloz, D., *et al.*, 2004, A&A, 423, 385

Rivera, E. J., Lissauer, J. J., Butler, R. P., *et al.*, 2005, astro-ph/0510508

Santos, N. C., Israelian, G., & Mayor, M. 2001, A&A, 373, 1019

Santos, N. C., Israelian, G., & Mayor, M. 2004, A&A, 415, 1153

Santos, N. C., Israelian, G., Mayor, M., *et al.*, 2003, A&A, 398, 363

Udry, S., Mayor, M., Naef, D., *et al.*, 2000, A&A, 356, 590

Tabachnik, S. & Tremaine, S. 2002, MNRAS, 335, 151

Wright, J. T., Marcy, G. W., Butler, R. P. & Vogt, S. S. 2004, ApJS, 152, 261

Zucker, S. & Mazeh, T. 2001, ApJ, 562, 1038

Tenth anniversary of 51 Peg-b : Status of and prospects for hot Jupiter studies
Proceedings of Haute Provence Observatory Colloquium (22-25 August 2005)
Edited by L. Arnold, F. Bouchy, and C. Moutou

Searching for planets around stars in wide binaries

S. Desidera[1], R. Gratton[1], R. Claudi[1], M. Barbieri[1], G. Bonanno[2], M. Bonavita[3], R. Cosentino[2,4], M. Endl[5], S. Lucatello[1], A. F. Martínez Fiorenzano[1,3], F. Marzari[6], and S. Scuderi[2]

[1] *INAF - Osservatorio Astronomico di Padova, Vicolo dell'Osservatorio 5, Padova, Italy [desidera@pd.astro.it]*

[2] *INAF - Osservatorio Astrofisico di Catania, Via S. Sofia 78, Catania, Italy*

[3] *Dipartimento di Astronomia, Università di Padova, Vicolo dell'Osservatorio 2, Padova, Italy*

[4] *INAF - Centro Galileo Galilei, Calle Alvarez de Abreu 70, Santa Cruz de La Palma, Spain*

[5] *McDonald Observatory, University of Texas at Austin, Austin, USA*

[6] *Dipartimento di Fisica, Università di Padova, Via Marzolo 8, Padova, Italy*

Abstract. We present the status of the radial velocity planet search on going at TNG using the high resolution spectrograph SARG. We are observing about 50 wide binaries with similar components, searching for planets and abundance anomalies caused by the ingestion of metal-rich planetary material. No clear planet detection emerged up to now. Evaluation of the statistical significance in terms of frequency of planets in binaries is in progress. The abundance analysis of half of the sample revealed no pair with large difference, allowing to place rather severe clues on the ingestion of metal-rich material during the main sequence lifetime of the stars.

1. Scientific motivations

The search for planets in multiple systems allows to improve our knowledge on planet formation and evolution. On one hand, the frequency of planets in binary systems has a strong effect on the global frequency of planets, more than half of solar type stars being in binary or multiple systems (Duquennoy & Mayor 1991). On the other hand, the properties of planets in binaries, and any difference with those of the planets orbiting single stars would shed light on the effects caused by the presence of the companions. The occurrence of some difference on the period-mass relation was indeed suggested (Zucker & Mazeh 2002). It is also possible that the binary companion of a planet host forces the planet to reach high eccentricities through the Kozai mechanism (Wu & Murray 2003).

Moreover, binarity can be used also to study the origin of the planet-metallicity connection (Fischer & Valenti 2005): if the ingestion of planetary material occurs, increasing the metallicity of the outer layer of the star, a chemical abundance difference between the components should be detectable. This is much easier to identify than a chemical anomaly in a normal field star, for which no proper reference is available.

With these two science goals, we started a radial velocity (RV) survey of the components of wide binaries. We are using SARG, the high resolution spectrograph of the TNG (Gratton et al. 2001), equipped with an iodine cell to derive high precision RVs.

2. The sample

The sample was selected from the Hipparcos Multiple Star Catalog, considering binaries in the magnitude range $7.0 < V < 10.0$, with magnitude difference between the components of $\Delta V < 1.0$, projected separation larger than 2 arcsec (to avoid contamination of the spectra), parallax larger than 10 mas and error smaller than 5 mas, with $B-V > 0.45$ and spectral type later than F7. About 50 pairs (100 stars) were selected.

The sample is then formed by wide binaries with mass ratio close to 1. Considering systems with similar components is crucial for the accuracy of the differential chemical abundance analysis. Fig. 1 shows the distribution of the projected separation in AU. For most of the pairs, it results between 50 and 600 AU.

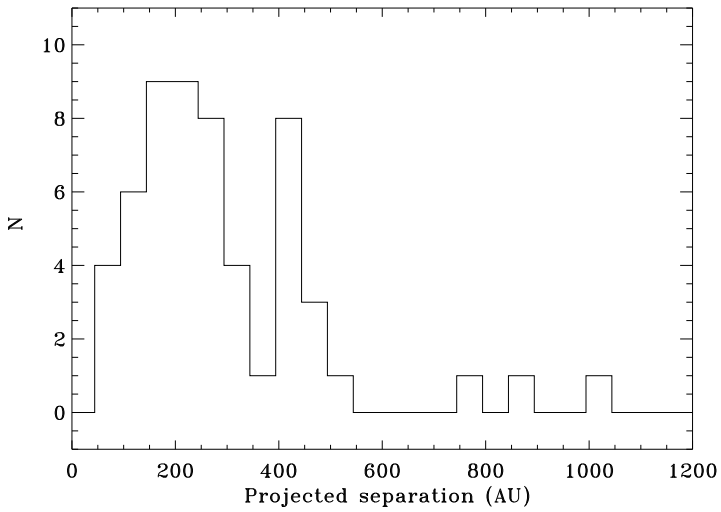

Figure 1. *Distribution of the projected separation in AU of the binaries in the sample.*

3. Abundance analysis

Differential abundance analysis was performed as described in Desidera et al. (2004a), reaching errors of about 0.02 dex in the iron content difference. We fully exploit the physical link between the components (same distance from the Sun), deriving effective temperatures difference from ionization equilibrium and gravity difference from the magnitude difference.

The analysis of 23 pairs, about half of the sample, shows that most of the pairs have abundance differences smaller than 0.02 dex and there are no pairs with differences larger than 0.07 dex. The four cases of differences larger than 0.02 dex may be spurious because of the larger error bars affecting pairs with large temperature difference ($\Delta T_{eff} \geq 400$ K), cold stars ($T_{eff} \leq 5500$ K) and stars with rotational velocity larger than 5 km/s.

Fig. 2 shows the amount of iron accreted by the nominally metal richer component to explain the observed abundance difference. For most of the slow-rotating stars warmer than 5500 K, characterized by a thinner convective envelope and for which our analysis appears to be of higher accuracy, this is similar to the estimates of rocky material accreted by the Sun during its main sequence lifetime (about 0.4 Earth masses of iron, Murray et al. 2001).

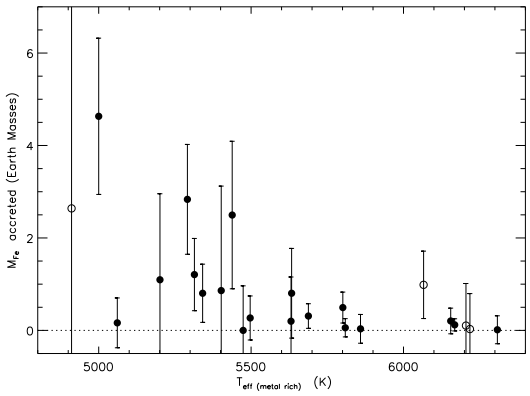

Figure 2. *Estimate of iron accreted by the metal-rich component of each pair as a function of its effective temperature, taking into account the mass of the mixing zone as in Murray et al. (2001). Empty circles: stars with significant rotation broadening, for which our analysis is less accurate. Filled circles: other stars. The less severe limits at lower effective temperatures are mostly due to the more massive convective zone of cool stars. The mass of meteoritic material is about 5.5 times the mass of iron.*

4. Radial velocities

RVs were determined using the AUSTRAL code (Endl et al. 2000) as described in Desidera et al. (2003). Typical errors are 2-3 m/s for bright stars observed as standards to monitor instrument performances and 5-10 m/s for the $V \sim 8 - 9$ program stars. 51 Peg was observed several times during the instrument commissioning and occasionally during the survey. The results are shown in Fig 3.

5. New triple systems

A by–product of our project is the detection of new spectroscopic binaries among the components of the wide binaries. These systems are then composed by at least three components. Some of these systems are presented in Desidera et al. (2005).

6. Stars with long term trends

About 10% of the stars in the sample show long term linear or nearly linear trends. In one case the trend is due to the known companion, as

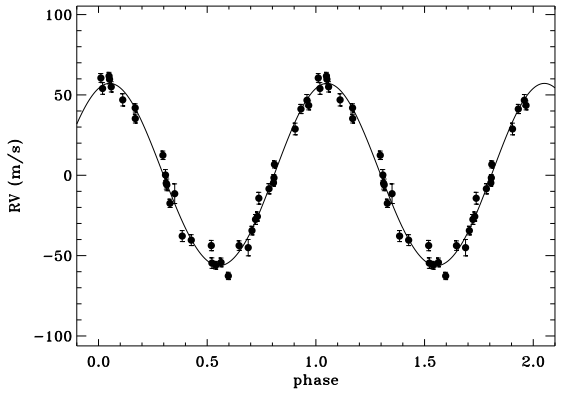

Figure 3. *Radial velocities of 51 Peg obtained with SARG phased to the orbital period.*

trends with opposite sign and nearly the same magnitude are observed for the two components. In the other cases the trends are due to low mass, possibly sub-stellar companions. Direct imaging to search for such systems is planned. The direct identification of sub-stellar objects as companions of stars for which age and chemical composition can be derived would play a relevant role in the calibration of models of sub-stellar objects.

7. Low amplitude variables and planet candidates

Some further stars show RV variability above internal errors. One case we investigated in detail is that of HD 219542B. The 2000-2002 data indicated a possible periodicity of 111 days with a significance of about 97% (Desidera et al. 2003). However, the continuation of the observations revealed that the RV variations are likely due to stellar activity (Desidera et al. 2004b). Other candidates, mostly of fairly low amplitude, are emerging from our sample. Further observations are in progress.

8. Line bisectors: a tool to study stellar activity and contamination

The relevance of activity jitter for the interpretation of the RV data prompted us to develop a tool to measure the profile of the spectral lines. The existence of a correlation between the variations of the RV

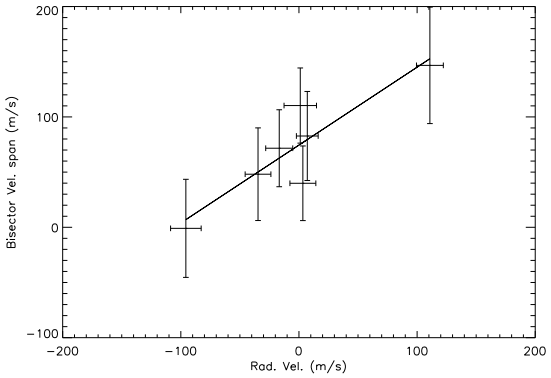

Figure 4. *Radial velocity - line bisector correlation for HD 8071B. This is likely due to the contamination by the companion HD 8071A*

and those of the line profile might indicate a non-Keplerian origin for the observed RV variations. Our approach allows to use the same spectra acquired for the derivation of RVs, removing the iodine lines by means of a suitable spectrum of a fast rotating early type star with the iodine cell in the optical path. The procedure is described in detail in Martinez Fiorenzano et al. 2005a (see also Martinez Fiorenzano et al. 2005b).

The study of line shape is relevant for our program also as a diagnostic for the contamination of the spectra by the wide companion. In the case of HD 8071B, we indeed observe a correlation likely due to the contamination of HD 8071A. We are confident that this is the worst case, as this pair is one of the closest in our sample (separation 2.1 arcsec) and the large amplitude RV variations of HD 8071A (Desidera et al. 2005) should increase the effect of a variable contamination of the observed RVs of HD 8071B.

9. Upper limits on planetary companions

While no confirmed planet detection emerged up to now from our survey, a detailed analysis of the negative results would allow to constrain the frequency of planets in binary systems. Since we are focusing on a specific type of binaries, wide binaries with similar components, such a study is complementary to other studies of planets in binaries (Eggenberger et al. 2005).

To this aim, we are deriving upper limits on the planetary companions still compatible with the observations. For period longer than

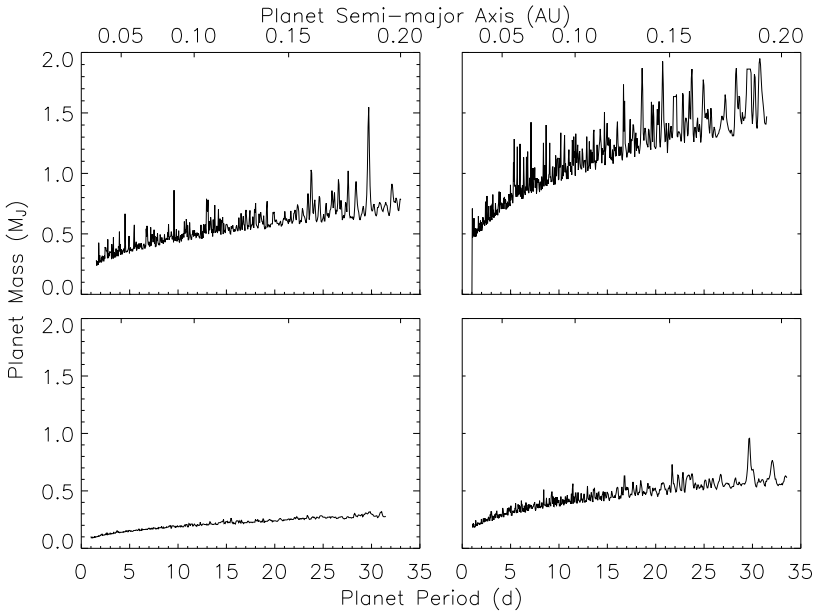

Figure 5. *Upper limits on planetary companion on short-period circular orbit for four stars representative of our sample. For the star on the upper-right corner planet detectability is strongly limited by stellar activity. The star in the lower-left corner is the one with the best limits, thanks to the low dispersion of RVs and the large number of measurements. The behavior of the other two stars is more typical for our survey.*

a few days, we consider eccentric orbits in our estimation, as described in Desidera et al. (2003).

Fig. 5 shows the upper limits on planetary companion on short-period circular orbit for four stars representative of our sample. The results of the upper limit for period in the range 3-4 days (the typical period of 51 Peg planets) is summarized in Fig. 6. We are able to exclude 0.3 M_J, 0.5 M_J and 1.0 M_J planets in 3-4 days orbit for 34%, 62% and 96% of the 71 stars with at least 10 observations. For such short period we consider only circular orbits, as observed for the most of the close-in planets detected up to now. A full statistical evaluation of the upper limits is in progress. This will allow to place constrain on the frequency of planets around the components of wide binaries with similar components.

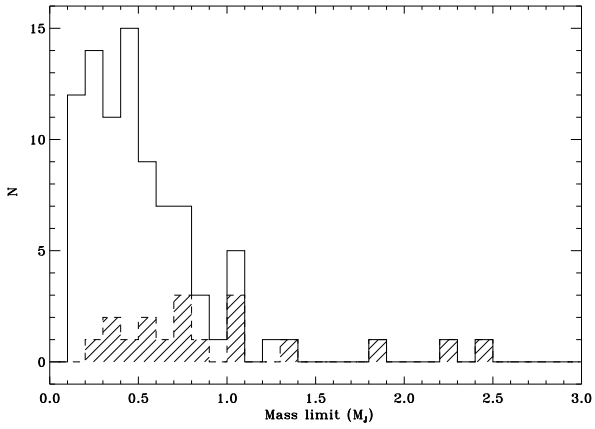

Figure 6. *Distribution of the mean upper limits between 3 to 4 days for the stars in our sample. The dashed region refers to stars with less than 10 measurements, the empty region to the other stars.*

Acknowledgements. This work was partially funded by COFIN 2004 'From stars to planets: accretion, disk evolution and planet formation' by Ministero Università e Ricerca Scientifica, Italy.

References

Desidera, S., Gratton, R., Endl, M. et al. 2003, A&A 405, 207

Desidera, S., Gratton, R., Scuderi, S. et al. 2004a, A&A, 420, 683

Desidera, S., Gratton, R., Endl, M. et al. 2004b, A&A, 420, L27

Desidera, S., Gratton, R., Claudi, R. U. et al. 2005, in Proceedings of ESO Workshop *Multiple stars across the HR diagram*, in press

Duquennoy, A., & Mayor, M. 1991, A&A, 248, 485

Eggenberger, A. et al. 2005, in Proceedings of ESO Workshop *Multiple stars across the HR diagram*, in press

Endl, M., Kürster, M., & Els, S. 2000, A&A, 362, 585

Fischer, D., & Valenti, J. 2005, ApJ, 622, 1102

Gratton, R., Bonanno, G., Bruno, P. et al 2001, Exp. Astr., 12, 107

Martinez Fiorenzano, A.F., Gratton, R., Desidera, S. et al. 2005a, A&A, in press (astro-ph 0508096)

Martinez Fiorenzano, A.F., Gratton, R., Desidera, S. et al. 2005b, this volume

Murray, N., Chaboyer, B., Arras, P. et al. 2001, ApJ, 555, 810

Wu, Y., & Murray, N. 2003, ApJ, 589, 605

Zucker, S., & Mazeh, T. 2002, ApJ 568, L113

Tenth anniversary of 51 Peg-b : Status of and prospects for hot Jupiter studies
Proceedings of Haute Provence Observatory Colloquium (22-25 August 2005)
Edited by L. Arnold, F. Bouchy, and C. Moutou

Planets of young stars: the TLS radial velocity survey

M. Esposito[1,2], E. Guenther[1], A.P. Hatzes[1], and M. Hartmann[1]

[1] *Thüringer Landessternwarte Tautenburg, Sternwarte 5, 07778 Tautenburg, Germany [mesposito@sa.infn.it]*

[2] *Dipartimento di Fisica "E.R. Caianiello", Università di Salerno, via S. Allende, 84081 Baronissi (Salerno), Italy*

Abstract. We report on the search for planets orbiting 46 nearby young stars performed at the State Observatory of Turingia (TLS) by means of a radial velocity survey. The aim of this program is to test the theories of formation/evolution of planetary systems. For 19(8) stars we can exclude planets with $M \sin i \geq 1$ M_J (5 M_J) and $P \leq 10$ days; we find 1 short period binary and 5 stars with long period RV-trend. One good young exo-planet candidate is presented.

1. Introduction

In the last ten years, thanks to high precision radial velocity (RV) measurements, more than 100 extrasolar planets have been found. The most important observational campaigns up to now have focused on old solar type stars because such stars present all the characteristics (small $v \sin i$, high number of spectral lines, low activity) to exploit the best potentialities of the RV technique.

The orbits of the extra-solar planets are strikingly different from those of our solar system: some of them have massive planets of extremely short orbital periods (so called "hot Jupiters" or "Pegasides"), while others exhibit very high eccentricities. These results have given a new strong impulse to the theoretical efforts to explain the formation and evolution of planetary systems. However, even the most fundamental questions are still open. How common are planetary systems? How do planets form? By core accretion or by gravitational instability in the disk. Where do they form? Close-in Jupiter mass planets can form

in situ, or do they have to form at a certain distance and then migrate inward? New insights should come from the determination of the orbital parameters for planets in early evolutionary phases. According to some scenarios the frequency of planets was initially much higher than is observed in old stars, as a substantial fraction of the planets might have been either ejected from the system, or have been engulfed in the host stars. Since capture of planets is highly unlikely, the frequency of planets of young stars ought to be higher than that of old stars. The aim of this survey is to find out by how much. Another issue we could address concerns the evolution of the orbital parameters. In particular it would be important to know whether close-in planets have round orbits when they form or eccentric orbits, which then get circularized by tidal interaction with the host star.

There is an additional reasons for searching for planets of young stars. As pointed out by Sudarsky, Burrows, & Hubeny (2003) even old exo-planets orbiting a solar-like star at 0.1 AU would have a temperature of up to 900 K, because they are heated by the star. A massive, isolated planet with an age between 10^7 to 10^8 yrs would also have a temperature of more than 800 K but this time because it is still contracting. For close-in young planets both effects would add up resulting in objects of spectral type early L or even late M, which would be only 5 to 7 mag fainter than the host star. The direct detection of these objects, especially in the infrared light, would be possible by means of interferometric observations as well as tracking down spectral signatures, giving access to fundamental parameters like temperature, radius and true masses.

The presence of spots and/or plaques in the photosphere of active stars changes the profile of spectral lines causing fictitious variations in the RV measurements (the so-called jitter). Not only this source of noise can mask the periodical variations which are the characteristic signature of the presence of a planet, but what makes it even worse is the fact that the presence of spots combined with the stellar rotation can itself introduce spurious periodicities in the radial velocity signal.This explains why young stars, which are supposed to be active, have so far been excluded from the major RV surveys for planets detection. However Paulson et al. (2002) monitored 82 stars in the Hyades (age $\sim$ 700 Myr) finding a significant correlation between simultaneous RV and R'_{HK} for only 5 stars. Indeed exactly to what extent the stellar activity can hinder the detection of exoplanets in RV measurement has not yet clearly assessed.

Weighing pros and cons we finally decided to undertake a RV survey of young stars.

2. The TLS radial velocity survey

Observations began in 2001. We monitored a sample of 46 young, nearby dwarf stars of late spectral type and took 1500 spectra of these up to now.

2.1 The instrumental setup

The observations have been carried out at the State Observatory of Turingia (TLS) using the 2m "Alfred Jensch" telescope which is equipped with a Coudé echelle spectrograph. We used the visual grism which cover the spectral region from 4660 to 7410 $\AA$ in 44 orders. With a slit width of 1.2 arcsec a resolution of $R = 67000$ is achieved. An iodine cell placed in front of the slit generates a very dense system of absorption lines superimposed onto the stellar spectrum, which provides a highly precise wavelength scale and at same time allows to measure the PSF in situ over the spectrum. Radial velocities (RV's) are measured by means of a software package called RADIAL developed at the University of Texas and McDonald Observatory, based on the methods described in Marcy & Butler(1992) and Valenti, Butler & Marcy(1995).

2.2 Characterization of the sample

The identification of bona-fide young post-T-Tauri stars near the Sun still is an open astrophysical issue (Jensen 2001). Recently many nearby associations of young stars have been recognized: TWA, β Pic, Tucana-Horologium, η Cha, AB Dor (Zuckermann & Song 2004). For such coeval stellar groups statistics considerations help to achieve reliable estimations of the common age. Unfortunately all those associations are located in the Southern hemisphere.Thus in selecting the sample of stars to survey we did the Hobson's choice and looked out for young 'field' stars.

One of the best indicators of young age, especially for G and K stars, is the presence of the lithium LiIλ6708 absorption line. The convective envelope of these stars brings the lithium in contact with the stellar core where the temperature is high enough to cause its burning. As a consequence the lithium in the stellar atmospheres is progressively depleted. The lithium abundances can thus be used as an age estimator. Fig. 1 shows the LiIλ6708 equivalent width (EW) as a function of the T_{eff} for the stars in our sample and, as a comparison, for the Pleiades (age $\sim$ 100 Myr). As can be seen for the stars of Pleiades, the LiIλ6708 EW scatters significantly for the same T_{eff}. Thus it is not possible determine the age for every single star in our sample precisely. Rather, in a schematic way, we can subdivide our sample in two groups, one having ages comparable to the Pleiades and the other consisting of older

stars. In fact, many stars in the latter group have been recognized as members of the Ursa Major association which is 300 Myr old (Soderblom & Major 1993) (500 Myr according to King & Schuler 2005).

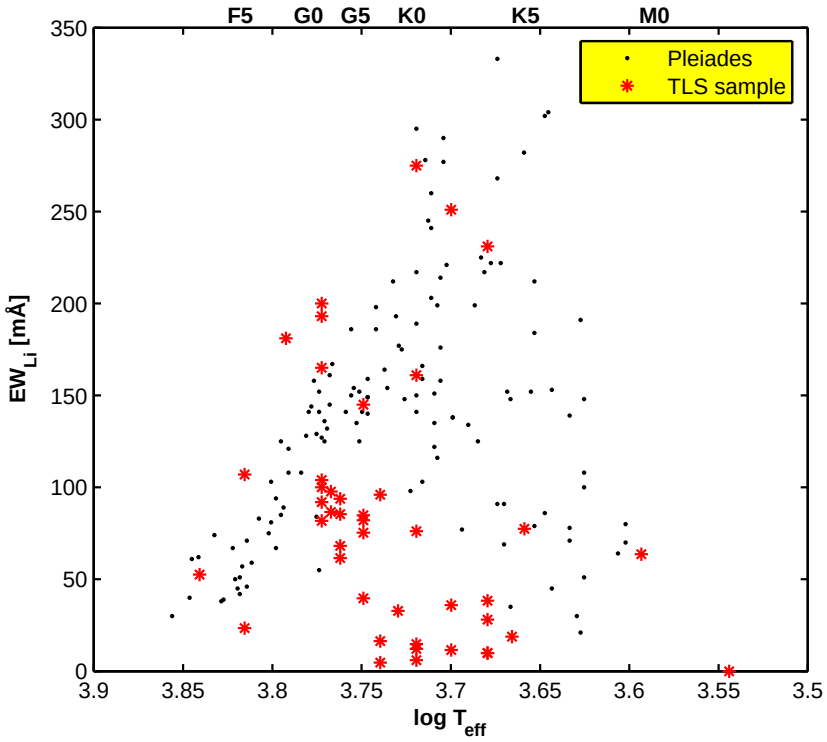

Figure 1. *Plot of the LiIλ6708 versus* $logT_{eff}$ *for the TLS sample and, as a comparison, for the Pleiades. Most of the star surveyed have ages comparable to the Pleiades (*$\sim$ *100 Myr); the clump with* $3.65 < logT_{eff} < 3.75$ *and* $EW < 50 m\AA$ *is probably made of* $300 - 500$ *Myr old stars (see text).*

Based on the Hipparcos parallaxes all our stars are at a distance of less than 50 pc from the Sun, and 36 of them are closer than 30 pc. Accordingly, they are relatively bright, ranging from the fifth to the ninth visual magnitude.

3. Analysis of the data

3.1 Internal errors

Fig. 2 (left panel) shows the average internal errors σ_{int} in the RV's as a function of the projected stellar rotational velocity $v \sin i$. As expected for rapidly rotating stars, the spectral lines broadening makes it difficult to achieve high precision RV values. However, up to a $v \sin i \leq 10$ km/s, we routinely get internal errors of 10 to 15 m/s .

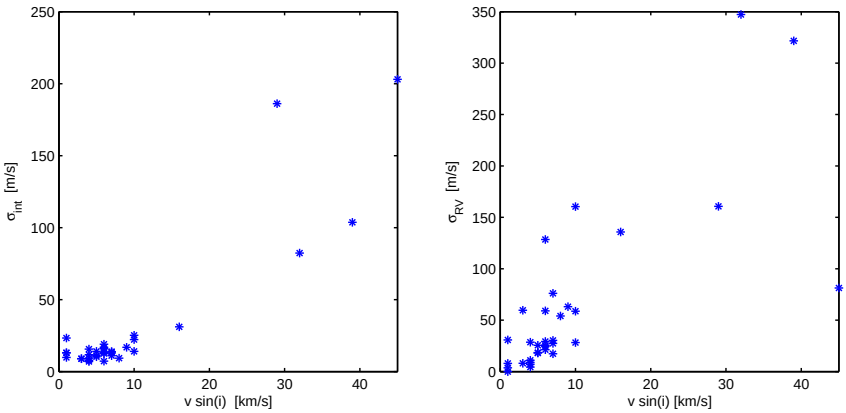

Figure 2. *(left) Plot of the average internal errors σ_{int} as a function of the stellar rotational velocity $v \sin i$. (right) σ_{RV} vs $v \sin i$; see the text for the definition of σ_{RV}. In this analysis only 34 stars have been considered excluding stars with less than 20 data points and stars which show clear RV-trend.*

3.2 RV-jitter

Apart from the fact that the RV's for rapidly rotating stars are more difficult to determine, these stars are also more active. In order to demonstrate this, we consider the σ_{RV} which is defined as the square-root of the difference between the standard deviation of the observed RV's (σ_{obs}) and the σ_{int} squared. σ_{RV} thus is a measure of the RV-variations presumably due to stellar activity. Fig. 2 (right) shows σ_{RV} against $v \sin i$. It can clearly be seen that stars of larger $v \sin i$ also show larger σ_{RV}-values. On the other hand the majority of stars in our sample which have $v \sin i \leq 10$ km/s show a σ_{RV} lower than 35 m/s. Such a level of 'noise' in the RV-measurements, even if larger than typical values for old dwarf stars of the same spectral type (Santos et

al. 2000), still allows the detection of a RV-signal of most of the known exo-planets. For instance, a planet with $M \sin i = 1\ M_J$ in a circular orbit around a 1 $M_\odot$ star with a period $P = 10(100)$ days induces a stellar wobble with a RV semi-amplitude of $K = 94(44)$ m/s which is larger than the scatter caused by activity for a star with a $v \sin i \leq 10$ km/s.

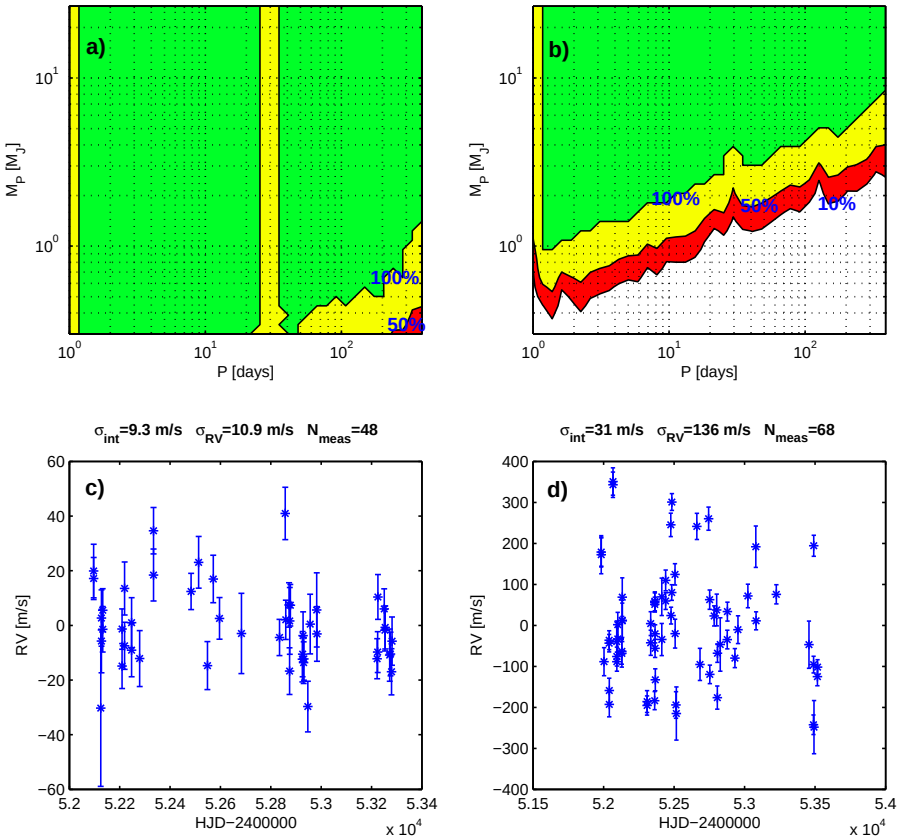

Figure 3. *(lower panels) RV vs HJD (heliocentric Julian date) for two stars showing a low (c) and high (d) level of jitter respectively. (upper panels) The detection limits in the mass-period diagram. Iso-probability curve for the 100%, 50% and 10% levels are plotted. In the upper grey zone (100%) we are virtually sure that a planet would have been detected.*

3.3 Detection limits

In order to derive upper limits for the detection of planets in our sample, we carried out simulations. For each point on a grid of values of the

orbital period P and the planetary mass $M \sin i$, assuming for the star a mass on the basis of its spectral type, we generate a sinusoidal RV curve. The curve is then sampled in the same way as the real data for that star, obtaining a set of simulated RV values.In the next step, we add noise of normal distribution to the data. The noise is scaled so that the σ of the simulated data is equal to the observed σ_{obs}. The whole procedure is repeated 5000 times, varying the phases randomly. For each of the 5000 simulated data-sets we then derive the value of the periodogram (S) for that period P (Scargle 1982) and thus obtain for a given P and $M \sin i$ a distribution of S, which is compared to a similar distribution for $M \sin i = 0$. If the two distributions do not overlap, we conclude that a planet of that P and $M \sin i$ can be excluded. Similarly, from the overlap of the two distributions, we can calculate the probability for excluding such planet.

The results of our simulations for two opposite cases are shown in Fig. 3. Quite remarkably in the best conditions (panel a) we easily would have been able to detect a planet with $M \sin i = 1 M_J$ for a period as large as 300 days. Besides, even in the worst case (panel b) thanks to the high number of data points ($N_{meas} = 68$) we are still sensible to very hot Jupiter-mass planets.

3.4 A young exo-planet candidate

In the whole sample we have found only three objects which show a long period RV trend compatible with the presence of a stellar companion and one young planet candidate. The RV data set for all these stars has been analyzed in the same way: we calculated the Scargle periodogram and in correspondence to the periods with higher peaks we estimate the weighted least squares best-fit orbital solution. The phase-folded RV curve for our candidate planet is shown in Fig. 4 together with the best-fit orbital parameters. As we know that RV variations can also be induced by stellar activity, we analyzed the Hipparcos photometry and found a P=1.6477 days periodicity. It is hence possible that the RV as well as the photometric variations originate from a $\sim$ 1.5 days stellar rotational period. However the star does not present enhanced X-ray luminosity and strong emission in the cores of the CaII H and K lines, which are typical of fast rotators, and the $v \sin i = 4$km/s would imply that we are observing the star almost pole-on. Further simultaneous spectroscopic and photometric observations will possibly confirm or discard the planet hypothesis.

Acknowledgements. M. Esposito's work was performed under the auspices of the EU, which has provided financial support to the "Dottorato di Ricerca Internazionale in Fisica della Gravitazione ed Astrofisica" of the Salerno University, through the "Fondo Sociale Europeo, Misura III.4".

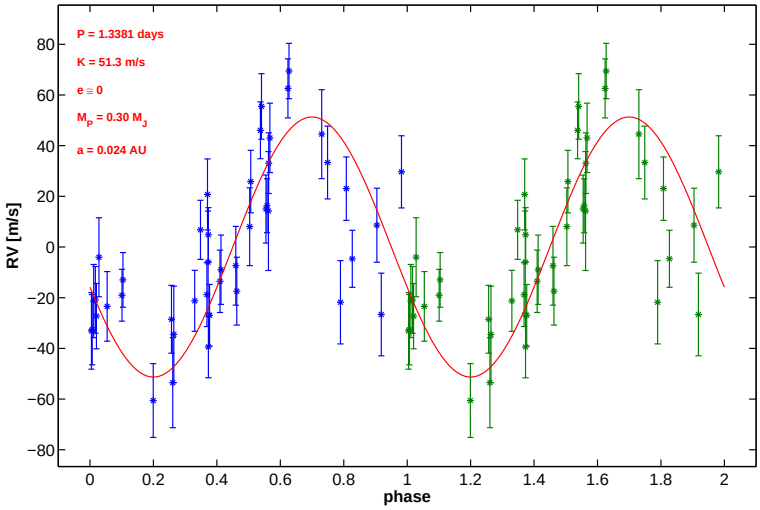

Figure 4. *The RV measurements for a G0 star in our sample phase-folded with a P=1.3381 days period. The best-fit RV curve and corresponding orbital parameters are reported.*

References

Jensen E.L.N. 2001, in ASP Conf. Ser. 244, Young Stars Near Earth: Progress and Prospects, ed. R. Jayawardhana & T.P. Greene (San Francisco: ASP), 3

King J.R. & Schuler S.C. 2005, PASP, 117 , 911

Marcy G.W. & Butler R.P. 1992, PASP, 104 , 270

Paulson D.B., Saar S.H., Cochran W.D., & Hatzes A.P. 2002 AJ124, 572

Santos N.C., Mayor M., Naef D., *et al.*, 2000, A&A361, 265

Scargle, J.D. 1982, ApJ, 263, 835

Soderblom D.R. & Major M. 1993, ApJ, 402 , 5

Sudarsky D., Burrows A., & Hubeny I. 2003, ApJ, 588, 1121

Valenti J.A., Butler R.P., & Marcy G.W. 1995, PASP, 107 , 966

Zuckermann B. & Song I. 2004, ARA&A, 42, 685

Tenth anniversary of 51 Peg-b : Status of and prospects for hot Jupiter studies
Proceedings of Haute Provence Observatory Colloquium (22-25 August 2005)
Edited by L. Arnold, F. Bouchy, and C. Moutou

Elodie metallicity-biased search for transiting hot Jupiters

R. Da Silva[1], S. Udry[1], F. Bouchy[2], M. Mayor[1], C. Moutou[2], F. Pont[1], D. Queloz[1], N.C. Santos[3,1], D. Ségransan[1], and S. Zucker[1,4]

[1] *Geneva Observatory, Switzerland [Ronaldo.Dasilva@obs.unige.ch]*

[2] *Laboratoire d'Astrophysique de Marseille, France*

[3] *Lisbon Astronomical Observatory, Portugal*

[4] *The Weizmann Institute of Science, Israel*

Abstract. Star hosting planets have been shown to be more metal rich than single stars of the solar neighborhood. We present here a metallicity-biased planet-search program on-going since 18 months at Haute-Provence Observatory with the ELODIE spectrograph, where the target sample are high metallicity stars. We use a cross-correlation technique for radial-velocity estimates, together with a photometric transit search performed with the 120-cm telescope at the Haute-Provence Observatory. This program has already conducted to the discovery of two new planets candidates orbiting HD 118203 and HD 189733, and to the confirmation of another one orbiting HD 149143.

1. Introduction

Stars hosting planets are significantly metal richer than field stars in the solar neighborhood and the probability of hosting a giant planet is a strongly rising function of the star metal content. We can expect that up to 25 - 30% of the more metal-rich stars ([Fe/H] > 0.2 - 0.3) host a giant planet. A new survey was started in March 2004 (Da Silva et al. 2005) at the Haute-Provence Observatory with the high-precision ELODIE fiber-fed echelle spectrograph, and the main idea is to bias the tar-

get sample toward high-metallicity stars. We use the cross-correlation technique for the radial-velocity and metallicity estimates. The mainly targets are giant planets with short periods (Hot Jupiters), the ideal candidates in the search for photometric transits.

A similar planet-search program was simultaneously started by the N2K consortium (Fischer et al. 2004) aiming at the detection of short-period planets orbiting metal-rich stars.

2. First results

From the survey we have started, two new short-period planet candidates were found. One orbiting HD 118203 has $P = 6.1355$ d, $e = 0.31$ and $m_2 \sin i = 2.1\,\mathrm{M_{Jup}}$ (Da Silva et al. 2005). A plot with the last RV measurements is shown in Fig. 1 (left), together with the derived solution. The phase-folded RV curve with the complete set of data points corrected for the observed linear drift is displayed in Fig. 1 (right).

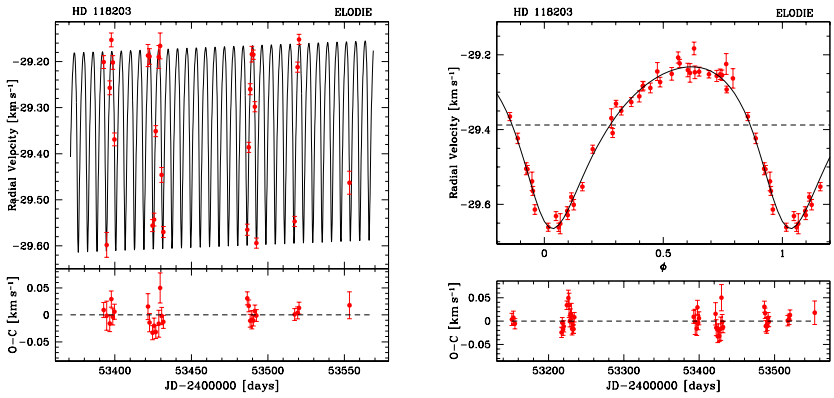

Figure 1. *Left: last 5-months RV measurements of HD 118203 with the best Keplerian + linear drift solution. Right: phase-folded RV after correction for the linear RV drift.*

The planet candidate around HD 189733 has $P = 2.219$ d and $m_2 \sin i = 1.15\,\mathrm{M_{Jup}}$ (Bouchy et al. 2005). Figure 2 (left) shows the RV measurements together with the derived Keplerian solution. From the ephemeris predicted by the RV, 3 transit events have been followed in photometry with the 1.20-m telescope at OHP. The first night, a complete photometric transit was observed in the B band (Fig. 2, right).

Fischer (2005) recently announced two new Hot-Jupiter detections around HD 149143 and HD 109749. HD 149143 is amongst the stars of our sample and its orbit has been confirmed (Da Silva et al. 2005).

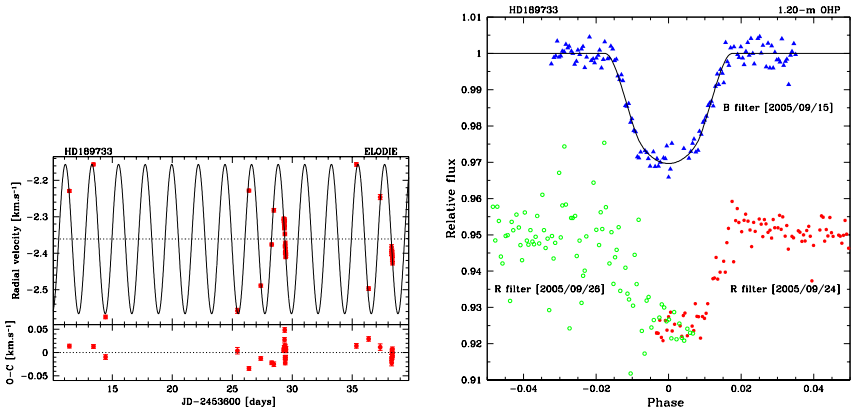

Figure 2. *Left: RV measurements of HD 189733 superimposed on the best Keplerian solution. Right: photometric transits observed with the 1.20-m OHP telescope. (figures from Bouchy et al. 2005)*

3. Conclusions

We have presented the new ELODIE planet-search program biased toward metal-rich stars and the first results of planetary detection: *(i)* a planet in a rather eccentric orbit around HD 118203, with $P = 6.1335$ d; *(ii)* a transiting Hot Jupiter orbiting HD 189733 with $P = 2.219$ d; *(iii)* and a Hot Jupiter around HD 149143, recently announced by the N2K project and confirmed by our program. The detection of 3 new planets in less than one year demonstrates the efficiency of the new program to find Hot Jupiter candidates.

Acknowledgements. We are grateful to the Swiss National Science Foundation, the Geneva University, the Haute-Provence Observatory (France), the Fundação para a Ciência e a Tecnologia (Portugal), and the Coordenação de Aperfeiçoamento de Pessoal de Nível Superior (Brazil).

References

Bouchy, F., Udry, S., Mayor, M., et al. 2005, A&A, 444, L15

Da Silva, R., Udry, S., Bouchy, F., et al. 2005, A&A, in press

Fischer, D.A., Valenti, J., & Marcy, G. 2004, in *Stars as suns: activity, evolution and planets, Proc. IAU Symp., 219, 29*

Fischer, D.A., *et al.*, 2005, these proceedings

Tenth anniversary of 51 Peg-b : Status of and prospects for hot Jupiter studies
Proceedings of Haute Provence Observatory Colloquium (22-25 August 2005)
Edited by L. Arnold, F. Bouchy, and C. Moutou

Radial velocity variations of G and K giants

M.P. Döllinger[1], L. Pasquini[1], A. Hatzes[2], A. Weiss[3], J. Setiawan [4], L. da Silva [5], J.R. de Medeiros [6], and L. Girardi [7]

[1] *European Southern Observatory, Karl Schwarzschild Strasse 2, 85748, Garching bei München, Germany [mdoellin@eso.org]*

[2] *Thüringer Landessternwarte Tautenburg, Sternwarte 5, D-07778 Tautenburg, Germany*

[3] *Max-Planck-Institut für Astrophysik, Garching bei München, Germany*

[4] *Max-Planck-Institut für Astronomie, Königstuhl 17, D-69117 Heidelberg, Germany*

[5] *Observatorio Nacional, R. Gal. Jose Cristino 77, 20921-400 Sao Cristavao, Rio de Janeiro, Brazil*

[6] *Departamento de Fisica, Universidade Federal do Rio Grande do Norte, 59072-970 Natal, RN, Brazil*

[7] *INAF-Osservatorio Astronomico di Trieste, Via Tiepolo 11, I-34131 Trieste, Italy*

Abstract. G and K giants are a new class of radial velocity (RV) variables. In order to reveal the reasons of this variability we started in February 2004 a program to observe a northern sample of 62 K giants from the Thüringer Landessternwarte Tautenburg (TLS) with the aim of using accurate radial velocity measurements to determine the fraction of K giants showing long-term and short-period variations. Our first results show a typical RV precision of 3 to 5 m s^{-1}. About 15% of the star sample exhibits long-term RV variations on time scales of several hundreds of days. Among these, for one program star we have a good time coverage, and the long-term variations may be due to a planetary companion.

1. Introduction

G and K giants are cool, evolved stars, which have moved off the main sequence. This sample span the entire Red Giant Branch (RGB) including the red clump and early-AGB phases. K giants are a class of variable stars with multi-periodic RV variations with different amplitudes and two categories of time scales. The fact that RV variability in giants has higher amplitudes (10 to 500 m s^{-1}) than that commonly seen in dwarfs, suggests that it results from some specific characteristics of these stars. The short-period variations (2 to 10 days) are likely caused by p-mode oscillations. In contrast the long-period RV variations occur on time scales of several hundreds of days and can be due to orbiting stellar/sub-stellar companions, but these require long-lived, and coherent RV variations that are not always observed. Doppler shifts caused by low mass companions are expected to be extremely stable with time. They should not induce any variations in the spectral line profile or be accompanied by variations in stellar activity indicators. We thus do not expect any correlation between radial velocity variations and bisector shape or chromospheric activity. By measuring the projected rotational velocity of the stars and estimating their radius we can also check that the orbital period differs substantially from the rotational period which will enable us to exclude rotational modulation. If a large surface inhomogeneity, passes the line-of-sight of the observer as the star rotates, then this causes distortions in the spectral line profiles and that will be detected as RV variation with the rotation period of the star.

2. Data analysis

Our spectra have been taken since February 2004 by using the high resolution Coudé Echelle Spectrometer (R=67,000) at the Alfred-Jensch 2m telescope in Tautenburg. We used an iodine absorption cell placed in the optical path in front of the spectrographs slit. The resulting iodine absorption spectrum is superposed on top of the stellar spectrum providing a stable wavelength reference against which the stellar RV is measured. RV's are calculated by modeling the observed spectra with a high signal-to-noise ratio template of the star (without iodine) and a scan of our iodine cell taken at very high resolution with the Fourier Transform spectrometer of the McMath-Pierce telescope at Kitt Peak. We compute the relative velocity shift between stellar and iodine absorption lines as well as we model the temporal and spatial variations of the instrument profile. The spectrum is split up in typically 125 chunks, where the values determined for each chunk. The achieved RV accuracy is 3 to 5 m s^{-1}.

3. Results

3.1 Statistics of the Tautenburg survey

- 11 stars (16 %) belong to binary systems
- 6 stars (9 %) are constant
- 9 stars (15 %) exhibit long-term RV variations which are possibly caused by low mass and planetary companions, rotational modulation and/or pulsations
- 36 stars (60 %) exhibit short-period RV variations due to oscillations.

3.2 Preliminary results on one K giant

One K giant shows long-term variations that may be due to a sub-stellar companion (Figure 1).

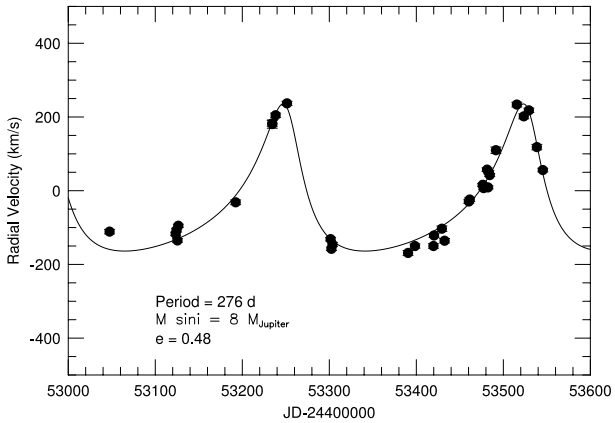

Figure 1. *RV variations of one Tautenburg star. The fit represents an orbital solution with P = 276 days, e = 0.48 and M sin i = 8 $M_{Jupiter}$.*

4. Conclusions

Although K giant variability can be complicated and can result from at least three mechanisms, the future aim of our survey is to distinguish between these mechanisms and to determine the frequency of planets around G and K giants as well as the full oscillation spectrum of the stars.

Tenth anniversary of 51 Peg-b : Status of and prospects for hot Jupiter studies
Proceedings of Haute Provence Observatory Colloquium (22-25 August 2005)
Edited by L. Arnold, F. Bouchy, and C. Moutou

51 Peg: a star with a second planet or a pulsating star?

M. Hrudková[1] and P. Harmanec[1,2]

[1]*Astronomical Institute of the Charles University, V Holešovičkách 2, CZ-18000 Praha 8, Czech Republic [mary@atrey.karlin.mff.cuni.cz]*

[2]*Astronomical Institute, Academy of Sciences, CZ-25165 Ondřejov, Czech Republic*

Abstract. The first determination of improved orbital elements of this star–planet system based on a combination of *all* available radial velocities of 51Peg is derived. A period analysis of the O–C deviations of the times of RV maxima from the new linear ephemeris shows a periodicity of $250^{\rm d}$ with a large amplitude of $0^{\rm d}.063 \pm 0^{\rm d}.005$. If interpreted as a light–time effect due to a third body in the system, this would imply an unrealistically large mass. Hence, one should seek other explanations like forced non–radial pulsations. However, it would be necessary to confirm or disprove the reality of the 250-d period via new dedicated observations.

1. A determination of orbital elements

51 Peg is the first solar–type star known to host a planetary companion. This was discovered by Mayor & Queloz (1995).

We compiled all available radial velocities (RVs hereafter) of 51 Peg known to us: RVs from spectra secured with the spectrographs AFOE (Whipple Observatory), ELODIE (CNRS), Gecko (CFHT) and Hamilton (Lick Observatory). The RVs span 9 years from 1994 to 2003. We used the program FOTEL (Hadrava 2004) to derive all solutions.

First we derived a solution where all RVs had the same unit weight. Using the computed rms (root mean square error of one measurement of unit weight) of individual datasets from this solution, we assigned each set a weight w proportional to $(\mathrm{rms})^{-2}$: $w = 1.0$ for ELODIE, $w = 4.47$ for Hamilton, $w = 0.46$ for Gecko and $w = 0.55$ for AFOE

spectra. In the final solution, these weights were applied. In Table 1, the final orbital elements are compared to those derived by Naef et. al. (2004) from the ELODIE data only. The Lucy & Sweeney (1971) test for possible non–zero eccentricity indicates a circular orbit within the limits of accuracy of current data. We therefore adopt the circular orbit, keeping in mind, however, that a very small eccentricity still cannot be fully excluded.

Table 1. *The final orbital elements of 51Peg. The solution by Naef et al. (2004) is shown for a comparison.*

Orbital elements		This work	Naef et al. (2004)
P	(d)	4.23081 ± 0.00005	4.23077 ± 0.00004
T	(HJD-2400000)	50195.447 ± 0.007	52497.000 ± 0.022
e		0 (fixed)	0 (fixed)
K_1	(m s^{-1})	56.7 ± 0.6	57.3 ± 0.8
rms	(m s^{-1})	7.6	11.8
$a_1 \sin i$	(10^{-5}AU)	2.21 ± 0.01	2.23 ± 0.03
$f_1(m)$	($10^{-10} M_\odot$)	0.80 ± 0.01	0.82 ± 0.03

2. The O–C analysis

We sorted the data in time and selected 22 suitable data subsets, most of them spanning no more than 30 days. Keeping the semi–amplitude and period fixed at the values from our final solution, we derived local epochs of maximum RV for each of them. Using the new linear ephemeris from our final solution, we then calculated the O–C deviations of these locally derived times of RV maxima. The corresponding O–C diagram is shown in Fig. 1 left.

We searched for a periodicity in the O–C values using Stellingwerf's (1978) PDM technique and found a period of 250 days as the best one. The interpretation in terms of the light–time effect due to a presence of a distant third body can safely be excluded since the semi–amplitude of the O–C deviations of $0^{\rm d}.063$ would imply an unrealistically large mass – see Fig. 1 right. Therefore, one has to think about the possibility that 51Peg is a pulsating star. We repeated all local sinusoidal fits for the $4^{\rm d}.23$ period, this time allowing also the convergency of semi–amplitudes of individual RV curves. Both, the O–C deviations and the semi–amplitudes were found to vary with the 250-d period.

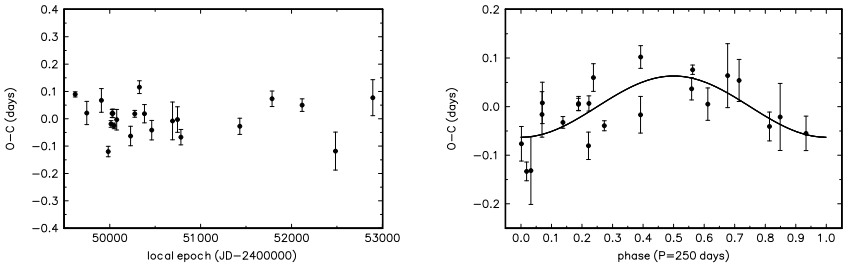

Figure 1. *The error bars shown are the rms errors of local epochs. Left: The O–C diagram of 22 locally derived solutions. Right: The O–C deviations plotted vs. phase of the 250-d period with K_1 value fixed. A sinusoidal fit to the data is shown by a solid line.*

If the 250-d period is a beat period of two close oscillations, then the candidate for the second oscillation period is either

$$4\overset{\mathrm{d}}{.}16032\ (4\overset{\mathrm{d}}{.}16^{-1} = 4\overset{\mathrm{d}}{.}23^{-1}+250\overset{\mathrm{d}}{.}00^{-1})$$
$$\text{or } 4\overset{\mathrm{d}}{.}30373\ (4\overset{\mathrm{d}}{.}30^{-1} = 4\overset{\mathrm{d}}{.}23^{-1}\text{-}250\overset{\mathrm{d}}{.}00^{-1}).$$

As non–radial pulsations were excluded by Hatzes et al. (1998) by the lack of the spectral variability, then the most likely explanation is that the $4\overset{\mathrm{d}}{.}23$ period is indeed the orbital period of a planet and the $4\overset{\mathrm{d}}{.}16$ or $4\overset{\mathrm{d}}{.}30$ period is a multiple of a synodic period or a forced oscillation.

However, one must be cautious about drawing conclusions from the second–order effects when combining disparate RV sets. The velocity amplitudes can vary between the sets and all RV's suffer from the night corrections. Rather then speculating further, we appeal to the observers having access to necessary instrumentation to obtain new series of RVs of 51Peg at different phases of the putative 250-d period.

Acknowledgements. We acknowledge the use of the program FOTEL from Dr. P. Hadrava. Drs. S. G. Korzennik, E. Shkolnik and G. A. H. Walker kindly provided us with their unpublished individual RVs of 51 Peg.

References

Hadrava, P. 2004, PAICz, 92, 1
Lucy, L. B. & Sweeney, M. A. 1971, AJ, 76, 544
Hatzes, A. P., Cochran, W. D., & Bakker, E. J. 1998, ApJ, 508, 380
Mayor, M. & Queloz, D. 1995, Nature, 378, 355
Naef, D., Mayor, M., Beuzit, J. L., *et al.*, 2004, A&A, 414, 351
Stellingwerf, R., F. 1978, ApJ, 224, 953

Tenth anniversary of 51 Peg-b : Status of and prospects for hot Jupiter studies
Proceedings of Haute Provence Observatory Colloquium (22-25 August 2005)
Edited by L. Arnold, F. Bouchy, and C. Moutou

Line bisectors and radial velocity jitter from SARG spectra

A. F. Martínez Fiorenzano[1,2], R. G. Gratton[2], S. Desidera[2], R. Cosentino[3,4], and M. Endl[5]

[1]*Dipartimento di Astronomia Università di Padova, Vicolo dell'Osservatorio 2, I-35122, Padova, Italy*
[fiorenzano@pd.astro.it]

[2]*INAF - Osservatorio Astronomico di Padova, Vicolo dell'Osservatorio 5, I-35122, Padova, Italy*

[3]*INAF - Osservatorio Astrofisico di Catania, Via S. Sofia 78, Catania, Italy*

[4]*INAF - Centro Galileo Galilei, Calle Alvarez de Abreu 70, 38700 Santa Cruz de La Palma (TF), Spain*

[5]*McDonald Observatory, The University of Texas at Austin, Austin, TX 78712, USA*

Abstract. We present an analysis of variations of bisectors of spectral lines for a few stars observed during the high precision radial velocity planet survey ongoing at SARG at TNG, and discuss the relation with differential radial velocities. The I_2 cell lines employed in the radial velocities measurements were used to improve the wavelength calibration and then removed before bisector analysis. The line bisectors were then computed from average absorption profiles obtained by cross correlation of the stellar spectra with a mask made from suitable lines of a solar catalog. The run of bisector velocity span against radial velocity was studied searching for correlations between line asymmetries and radial velocity variations. A correlation was seen for HD 166435 due to stellar activity and for HD 8071B due to spectral contamination by the companion. No correlation was seen for 51 Peg and ρ CrB, stars hosting planets. We conclude that this technique may be useful to separate radial velocity variations due to center of mass motion from spurious signal in spectra acquired with the I_2 cell.

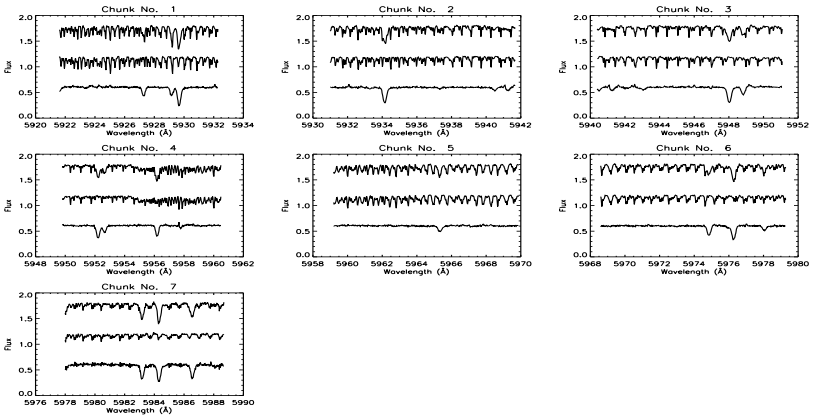

Figure 1. *Spectrum of HD 166435. Upper spectra is from the star with I_2. In the middle are spectra of the B-star with I_2. Lower spectra is free of I_2 after dividing the star by the B-star spectra.*

1. Spectra

We analyze spectra in the range 4580-6170 Å. Spectral orders were divided in 7 chunks of ∼10 Å. The spectrum of a B-star, for the radial velocity (RV) determination, was employed to remove the I_2 lines superposed to the stellar spectrum for calibration in λ (see Figure 1).

2. The Cross Correlation Function (CCF)

To compute the CCF a mask is constructed from the solar catalog by Moore et al. (1966), selecting lines separated by $\geq$ 0.1 Å, intensity of 3 to 30 Fraunhofer, well defined, without blends and avoiding telluric features. The mask is a sum of δ functions: 1 for the selected λ and 0 elsewhere. The CCF is computed for every chunk, multiplied by a weight, added and normalized.

3. The line bisector

A line bisector (LB) is the mid point of the profile. The bisector velocity span (BVS) is the velocity difference between two zones of the profile: one near the wings (Top) and the other near the core (Bottom). These zones were determined for the most significant correlation in the case of HD 166435, i.e., Top centered at 25% of the absorption depth, Bottom at 87% and both of 25% width. The same percentages were considered for all stars to be consistent in the analysis (for details see Martínez Fiorenzano et al. 2005).

4. Analysis

RVs are computed using AUSTRAL (Endl et al. 2000, Desidera et al. 2003). LBs are computed from the same spectra with an IDL code (Martínez Fiorenzano et al. 2005). We find a correlation between BVS and RV for HD 166435 as Queloz et al. (2001), and for HD 8071B likely due to spectral contamination from the companion. It is a member of a visual binary system and the primary has the smallest projected separation (2.1″) in the sample of the survey. For 51 Peg and ρ CrB the line bisectors show a constant shape and no correlation between BVS and RV.

5. Conclusions

We studied the variation of LBs in the same spectra acquired through the I_2 cell, employed for high precision RV measurements. We found that such variation, as measured by the BVS, shows spreads fully consistent with internal errors, as determined from photon statistics, spectral resolution and intrinsic line profiles. A significant correlation of BVS and RV was established in two cases: an anticorrelation for HD 166435, as found by Queloz et al. (2001), due to stellar activity, which makes the core of the profiles change from positive to negative values of RV. A positive correlation for HD 8071B, due to contamination of light from the companion star producing an asymmetry in the red wings of the profiles with an inclination of the LBs toward positive RVs. For the stars known to host exoplanets, 51 Peg and ρ CrB, no correlation was found, further supporting the conclusion that RV variations are due to Keplerian motion. We conclude that spectra acquired using the I_2 cell may be used to study variations of line bisectors. In order to achieve the required accuracy, it is necessary to deal with high quality spectra, high S/N to reduce error bars of BVS, or to study spectra where the RV variations are of large amplitude.

References

Desidera, S. et al. 2003, A&A, 405, 207

Endl, M. et al. 2000, A&A, 362, 585

Martínez Fiorenzano, A. F. et al. A&A, in press (astro-ph/0508096)

Moore, C. E. et al. 1966, The solar spectrum 2935 – 8770 Å (USGPO)

Queloz, D. et al. 2001, A&A, 379, 279

Tenth anniversary of 51 Peg-b : Status of and prospects for hot Jupiter studies
Proceedings of Haute Provence Observatory Colloquium (22-25 August 2005)
Edited by L. Arnold, F. Bouchy, and C. Moutou

Searching for planets around metal-rich stars

M. Hartmann[1], A.P. Hatzes[1], E.W. Guenther[1], and M. Esposito[1,2]

[1] *Thüringer Landessternwarte Tautenburg, Sternwarte 5, 07778 Tautenburg, Germany [michael@tls-tautenburg.de]*

[2] *Università di Salerno, via S. Allende, 84081 Baronissi (SA), Italy*

Abstract. We surveyed a small sample of metal-rich solar-like stars in our planet search program during the last 3 years. Here we present the detection of a brown dwarf and 3 long-period massive planet (or brown dwarf) candidates as well as one short-period planet candidate with $m \sin i \sim 0.1\ M_{Jup}$. Furthermore, we calculated the upper mass limits of possible companions for the other stars.

1. Introduction

Various studies (e.g. Santos et al. 2004) imply that the frequency of planets depends on the metallicity of their host stars. This result has been used as a strong argument for the core accretion scenario. In the previous studies large samples of stars have been observed, which necessarily limited the number of observations per star. Additionally, mostly single and inactive stars were observed.

Here we present a new study in which we selected a rather small sample of only 33 metal-rich stars, but took $\sim$ 1400 radial velocity (RV) measurements of these. The sample has a median metallicity of [Fe/H] = 0.23. We did not exclude active stars nor binaries. If the metallicity effect is real, we expect to find 8–9 stars with planets. However, for 6 of these stars it was already known that they have planets, we thus observed only the remaining stars. Since it was claimed that the detection of planets is easier for metal-rich stars than for metal-poor ones, we also added 8 stars of low metallicity to the target list as a comparison sample.

2. Observations and RV-measurements

The search for extrasolar planets around metal-rich stars is one part of the Tautenburg planet search program which started in 2001. For the project we use the 2.0-m Alfred Jensch telescope of the Thüringer Landessternwarte which is equipped with a high resolution Coudé Echelle Spectrograph (resolving power R = 67,000) and an iodine absorption cell which is placed in the optical light path. The accuracy achieved in our RV-measurements is shown in Figure 1 (left).

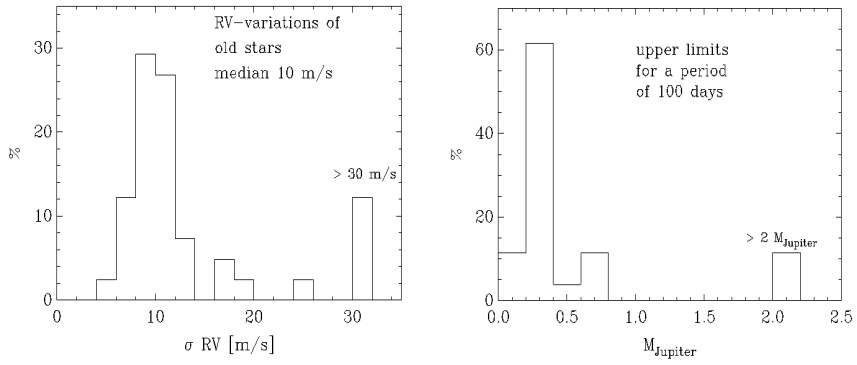

Figure 1. Left*: histogram of the achieved accuracy in the radial velocity measurements;* Right*: upper limits of the masses calculated for a period of 100 days and circular orbits.*

3. Results

The first sub-stellar companion discovered in this sample was a brown dwarf with a minimum mass of 26 M_{Jup}, moving in an eccentric orbit ($e = 0.4$) with a period of 798 days around the star HD 137510 (Endl et al. 2004). We also found three massive planet (or brown dwarf) candidates, all of them have periods larger than 3 years (see Figure 2). Additionally, there is one short-period planet candidate with $m \sin i \sim 0.1\ M_{Jup}$ in the sample. Apart from these findings, no other planets with $m \sin i \geq 0.5\ M_{Jup}$ and periods less than 3 years were found.

For all stars except the double stars, the 3 stars with the long-period candidates, and the brown dwarf host star, the upper limits of the masses were calculated for a period of 100 days and circular ($e = 0$) orbits (see right Figure 1). As shown in this histogram, for more than 70% of the observed stars (metal-rich and metal-poor sample) a planet with $m \sin i \geq 0.6\ M_{Jup}$ can be excluded.

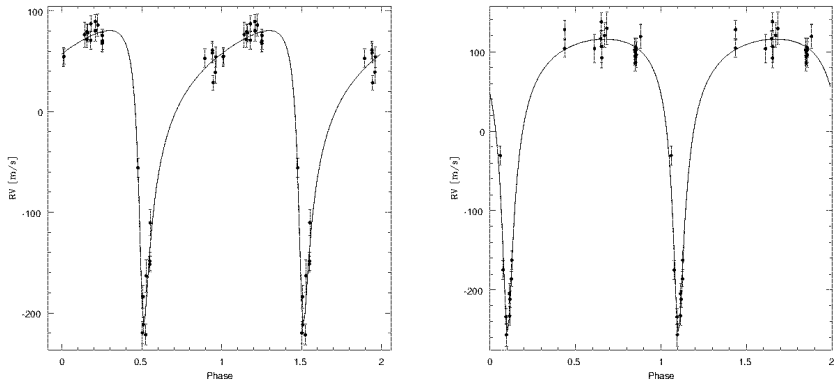

Figure 2. *Phase-folded radial velocity measurements of two massive planet (or brown dwarf) candidates, both with periods larger than 3 years. The masses of these objects are* $m \sin i \geq 5\ M_{Jup}$ *(left) and* $m \sin i \geq 7\ M_{Jup}$ *(right). The solid line represents the best-fit Keplerian orbital solution.*

4. Conclusions

From 33 stars of the metal-rich sample, 6 stars were already known to harbor planets. Together with our detected brown dwarf and the 3 long-period massive planet (or brown dwarf) candidates, there are in total 10 massive companions in this sample. Thus, the percentage of sub-stellar companions amounts $\sim$ 30% in good agreement with the results from Santos et al. (2004). Amongst the 8 stars of the comparison sample no planets were found.

Acknowledgements. We are grateful to the user support group of the Alfred Jensch telescope, especially B. Fuhrmann, J. Haupt, Chr. Högner, M. Pluto, J. Schiller, J. Winkler. We acknowledge STARLINK and IRAF software for preparing the observations and for analysing the data.

References

Endl, M., Hatzes, A. P., Cochran, W. D., McArthur, B., Allende Prieto, C., Paulson, D. B., Guenther, E. W., & Bedalov, A. 2004, ApJ, 611, 1121

Fuhrmann, K. 2004, Astron. Nachr., 325, 3

Santos, N. C., Israelian, G., & Mayor, M. 2004, A&A, 415, 1153

Taylor, B. J. 2003, A&A, 398, 731